JOURNAL OF MATERIALS SCIENCE **37** (2002) 1–28

Review
Structure and properties of glass-like carbon

L. A. PESIN
Department of Physics, Chelyabinsk State Pedagogical University, Lenin av., 69, Chelyabinsk, 454080, Russia

The comparison and discussion of the results of the long-term studies in the field of the glass-like carbon electronic and emission properties are presented. The data available from wide range of references and original experiments have given an opportunity to propose a new model of the glass-like carbon microcrystalline structure and its modification due to heat treatment.

1. Introduction

Glass-like carbon (GC) is a unique carbon material. It is a macroisotropic microcrystalline solid, which density comes to approximately 60% of that for monocrystalline graphite and thus indicates its high porosity. However, the practically complete absence of opened pores causes its chemical inertness even to active oxidizers. It makes GC an irreplaceable material for manufacturing constructional products that would work in aggressive environments and at high temperatures like chemical utensils, elements for emission electronics, and prosthetic appliances.

This obvious practical importance and unusual properties were attractive to scientists all over the world, particularly in France, Japan and the US. Hence there exist numerous publications mostly ranged between 1957 (the first discovery of cellulose-based GC in UK) and the beginning of the last decade. Since that time the situation has changed drastically; the stream of original papers became considerably weaker while the patents remain abundant. One may suggest some probable explanations of this fact. First of all, the nanoscale carbon structures, fullerenes and tubulenes, have been discovered. Their properties appeared to be extremely exotic and fascinating and the possibility of applications seemed to be exceptionally wide and hopeful. That is why these structures have drawn attention of many scientists working in the area of the carbon research. Others began to explore prospective carbon composites, including those based on GC or containing it as an important component. As all the previous studies gave a lot of information about the structure and properties of GC, it became possible to utilize it in practice. This is represented in numerous patents. Finally, certain interesting results of the GC studies made some researchers start broader and more comprehensive investigations involving various carbon materials and techniques. Thus, at the end of the nineties, when the GC studies seemed to have been done for the most part, there might come the prime time for writing comprehensive reviewing articles and books. The necessity for this kind of publications is evident. The results of the previous studies are sometimes controversial. So it is natural to compare and analyse them within one frame of reference and to find out, what in GC science is well established and rigorously confirmed, what appeared to be completely wrong, and what remains ambiguous and therefore requires further studies. The incompleteness of our knowledge about GC is obviously seen just from the absence of the unique exhaustive model for its structure: at present at least three *alternative* structural models coexist and are widely used for data interpretation.

According to one of them [1] GC crystallites are formed by stacks of *narrow* graphite-like layers. These carbon ribbons are entangled in a very quaint manner, transform into each other, are stratified in some separate ones, and merge in one ribbon with others, forming a complex polymer-like structure. The spaces between the stacks form micropores of various configurations and sizes. Such structure of crystallites reflects the features of thermosetting resins structure (such, for example, as phenol formaldehyde or phenol furfural formaldehyde resin), which are commonly used as precursors for GC synthesis. The rigidity of this structure makes it resistant to heat treatment: the spatial arrangement of the stacks is defined by the orientation of primary chains of the initial polymer and does not vary even when affected by the very high temperatures (up to 3000°C). This is a reason to refer GC to the class of non-graphitizable or hard carbons. Nevertheless, there is a monotonous increase of the carbon ribbons width with the elevation of the annealing temperature. Hence this effect makes it possible to study the influence of the width of an *anisotropic* carbon layer on various physical properties of GC. Bends and interlacing of carbon ribbons create a variety of valence angles and types of interatomic bonds in this material.

In contrast, the alternative models of "crumpled sheets" suggested by Oberlin [2] and of closed pores introduced by Shiraishi [3] postulate the existence of practically *isometric*, but heavily crumpled graphite-like sheets; heat treatment regularly reduces these layer distortions.

The model introduced by Shiraishi describes the structure of GC heat treated to high temperatures (about 2800°C). Its characteristic feature is a predominance

of closed pores forming the bulk of the material. This makes it quite distinct from Oberlin's model in prediction of different macroscopic properties (such as gas permeability, hardness, chemical reactivity, and so on). However, according to the spatial scheme given by Shiraishi, the shape of pore walls resembles crumpled or folded sheets very much. It means that the both models can lead to the similar description of microscopic parameters (magnetic susceptibility, thermoelectricity, electrical resistance, and so on). In this particular aspect one could expect a close similarity of the models suggested by Oberlin and by Shiraishi: both suggest similar layer defects effecting in the same way on the character of a carrier transport across the layer.

None of the models explains *all* the numerous data obtained up to now. Thus, their refinement and/or considerably deeper insight into the nature of carbon atoms bonding in GC are required. Clearly, this is impossible without summarizing the results of the previous studies and performing their critical analysis.

Unfortunately, only few reviews on GC are available. One of them is a very thoughtful and detailed but rather ancient (1976) book by Jenkins and Kawamura [4]. The other one is much briefer but relatively recent (1991) publication by Otani and Oya [5]. Both are closely related to the problems of GC structure and some of its properties. One should also mention a chapter in the book by Fialkov [6]. Besides, there are brilliant contributions by Fitzer *et al*. [7] and Oberlin [8] in *Chemistry and Physics of Carbons*. Some others [9–11] contain less direct information about GC, though the common features of hard carbons that are considered there are important for better understanding of the GC behaviour under heat treatment.

Though very distinct in details, all these reviews [4–11] have a common feature: they scope predominantly the structural and chemical aspects and/or the properties determined by the atomic arrangement. These books and chapters cover more or less thoroughly the GC fabrication process (including possible mechanisms of pyrolysis), its macro- and microstructure, chemical, mechanical (hardness, elasticity, etc.) and thermal properties, and the GC applications in different areas. On the contrary, the electrical properties are covered insufficiently. So called "electronic properties", such as Hall and Seebeck effects, magnetoresistance, magnetic susceptibility as well as spectroscopic data are not discussed at all. Hence at present there is no review article or book dealing with those properties of GC that are "governed" by the character of the electron energy distribution in the most direct way.

The present situation looks like following: the purely structural and chemical studies failed to give enough direct proofs in favour of any of the existing models of the GC structure. But one can try to use a "side route" based on the well-known high sensitivity of electronic structure to the features of atomic arrangement. Hence the analysis of the data on the studies of electronic properties as well as of various types of electron and photon emission can give a lot of information about GC energy bands. It may become now an extremely important tool in further attempts to get correct understanding of this fascinating carbon material.

This is the main aim and scope of the present article, and the author hopes it will be useful as the first collection, comparison and discussion of the results of the long-term studies in the field of the GC electronic and emission properties. The author and his co-workers accomplished a number of these studies. For the purpose of these studies a series of samples was specially synthesized. The series was obtained by carbonization of phenol formaldehyde resin at 1200°C (sample 1); this material was then exposed to the step heat treatment in inert atmosphere at 1500, 2000, 2500, 2700 and 3000°C during an hour at each temperature (samples 2–6 respectively). The author will use this enumeration of the samples when describing his own investigations and their results.

Sometimes dealing with the articles devoted to heat treated carbons it is not very simple to distinguish at once what kind of temperature is meant in any particular case: the temperature at which a studied parameter was measured or the heat treatment temperature of a carbon sample. So that readers could not confuse in any way ambient (or measurement) temperature and the maximum temperature of heat treatment (or annealing) the absolute scale (Kelvin) will be used in the first case and the centigrade scale (degrees centigrade) in the latter one.

2. Crystalline structure

Various techniques are used for studies of GC crystalline structure. Among them are wide angles X-ray diffraction [see, for example, [12–19], high-resolution electron microscopy [1, 13, 20, 21], neutron and electron diffraction [22–25] and small angles X-ray diffraction [21, 23, 26]. The analysis of a set of the results obtained by these techniques in most cases gives qualitative confirmation of the described above models of GC structure, though sometimes cannot completely exclude both supplementary and detailing ones as well as alternative models. As structural aspects are well reflected in the previous reviews [4–11] here only brief considerations are given but emphasizing the peculiarities not mentioned about before.

2.1. Wide angles X-ray diffraction

Rousseaux and Tchoubar [12, 13] have investigated GC samples heat-treated at temperatures in the range 1000–2700°C. The development of carbon layers [12] and the character of their mutual ordering [13] were studied. It has appeared that the profiles of (*hk*) reflections correspond to the model of flat rectangular anisotropic coherently scattering domains (CSD). These domains Rouseaux and Tchoubar identify as rather flat sites of the long but bent and folded carbon ribbons. The sizes of these sites are characterized by the parameters l_0 (in a direction of a primary carbon chain of initial resin) and L_0 (in a polymerization direction, Fig. 1). The heat treatment results in anisotropic growth of CSD. Up to heat treatment temperature (HTT) 2000°C l_0 is equal to 4 nm and does not vary, while L_0 grows from 4.5 nm at 1000°C up to 10 nm at 2000°C. In the HTT interval between 2000 and 2700°C parameter l_0 also practically

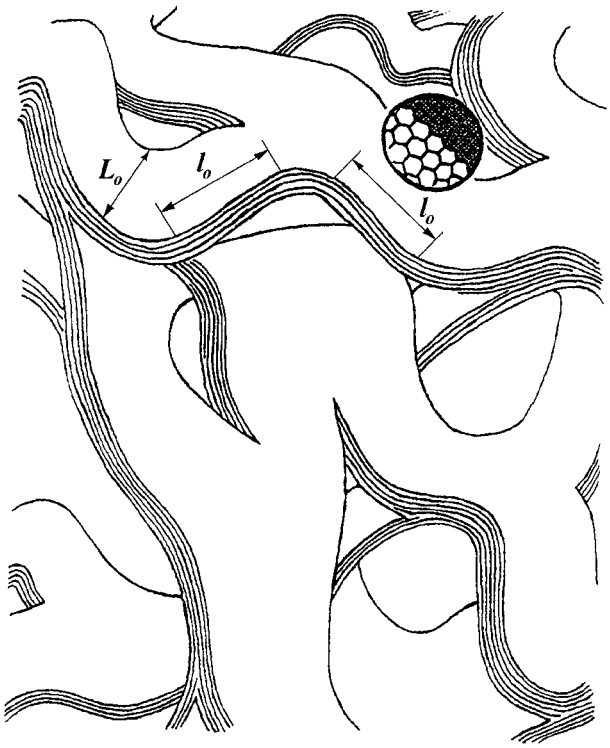

Figure 1 A spatial scheme suggested for the GC heat treated at 2700°C. L_0 and l_0 are respectfully the dimensions of a quasi-flat region of a fibril in two directions (adapted from [13]).

does not vary, reaching the maximum value of 4.5 nm; the changes of L_0 stop as well. Distortions of carbon rings are also strongly anisotropic: they are significant in directions parallel to an axis of a primary chain and much weaker in a polymerization direction. Thus, according to [12], parameter l_0 characterizes a mean distance between the folds of a ribbon, and the size L_0 corresponds to an average width of carbon layers. One should note, that these parameters were deduced by an extrapolation of side sizes of a rectangular model site l_{hk} and L_{hk} with which the calculated interference function for the definite h and k matches experimental one in the best way. Both l_{hk} and L_{hk} monotonously grow in the whole interval of HTT up to 2700°C.

The investigations of (*002*) and (*004*) X-ray reflections [13] has shown the advantages of reconstruction of a diffraction pattern from structural model (indirect method) in comparison with the Fourier analysis of experimental profiles (direct method). Rouseaux and Tchoubar determined the important parameters of GC crystalline structure: average number of layers in a ribbon, the mean distance between the layers, the average square of layer displacement [13]. These data show that the first of these parameters monotonously grows from 3 up to 7 with increase of HTT from 1000 to 2700°C. Interlayer spacing data were obtained from (*002*) and (*004*) diffraction maxima angular positions independently and essentially differ both in absolute values and in a course of HTT dependence. The analysis of (*002*) reflections shows sharp reduction of interlayer distance from 0.357 to 0.348 nm between 1000 and 2000°C and then weak recession down to 0.347 nm at 2700°C. On the contrary, angular positions of (*004*) reflection testify to growth of interlayer distance from 0.339 up to 0.344 nm during heat treatment in the range 1000–

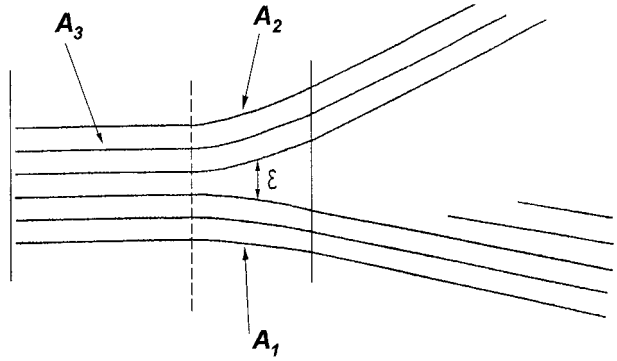

Figure 2 A scheme of a retrogression point between carbon layers stacks (from [13]).

2700°C. This striking discrepancy is explained in [13] by the presence of "retrogression points", i.e. defects of mutual arrangement of layers in a carbon ribbon resulting in its stratification in two separate ones (Fig. 2). The results obtained from the analysis of the higher order reflections correspond to the domain A_1, while the values determined from (*002*) reflection match to averaging on the whole set of the domains $A_1 + A_2 + A_3$ (Fig. 2). Thus, a mosaic character of the layers packing influences significantly on the angular position of (*002*) reflection and can be evaluated by the size ε. Rousseaux and Tchoubar [13] succeeded to estimate this parameter (0.36 nm) in GC sample with HTT = 2700°C. They confirm the existence of these defects by microphotos, where the carbon layers are distinctly resolved and the "retrogression points" are well observed. Heat treatment reduces the domains disorder and, accordingly, parameter ε, that results in the apparent interlayer distance reduction, but the real space between the next layers in one stack grows in the course of annealing.

This phenomenon is unique and is realized, apparently, only in GC. In graphitizable forms of carbon the thermal influence results simultaneously in reduction of disorder and in approach of carbon layers to each other [27]. Later when giving the analysis of the electronic properties of GC we shall still return to discuss this phenomenon.

Rousseaux and Tchoubar [13] have also shown that carbon layers in the stacks are not located equidistantly but there are variations of interlayer spaces. These variations are usually characterized by an average square of the layers displacement. Its value was determined independently from the analysis of (*002*) and (*004*) reflections. These two sets of data are in excellent mutual accordance and show the reduction of this parameter in the course of GC heat treatment.

Rousseaux and Tchoubar used the information obtained in [12, 13] from the analysis of (*10*), (*110*), (*002*), (*004*) reflections and electron microscopy data for specification of a spatial model of GC crystalline structure previously suggested in [1, 20]. The model is shown in Fig. 1. The bends of ribbons perturb a lattice mainly in the direction of initial polymer chains, the CSD growth occurs perpendicularly to the chains. The layers consist of quasi flat rectangular sites, which are strongly disordered relative to each other. These sites produce X-ray coherent scattering and are significantly smaller than the actual size of the layers. The model allows to

explain uniformity, impermeability to gases, pore configurations, corresponds to diamagnetic susceptibility and electrical resistance measurements [13].

The detailed analysis of diffraction profiles was not the scope of works done by Fischbach [14] and Saxena and Bragg [15]. X-ray diffraction patterns of GC samples were used only for definition of the average sizes of CSD with the help of standard Warren and Scherer routine. These mean parameters (the crystallites diameter L_a and height L_c) were involved for the interpretation of the results of diamagnetic susceptibility measurements [14] and for the estimation of activation energy necessary for GC structural modification due to heat treatment [15]. The analysis carried out in [14] has shown an essential difference in the dependence of diamagnetic susceptibility on L_a for soft carbons and GC. It has brought Fischbach [14] to a conclusion about various size distributions of crystallites and about different physical meaning of parameter L_a for soft and hard carbons.

Samples of GC heat treated between 1000–2800°C were studied in [15]. The (*002*) reflection was used for evaluation of the mean interlayer distance d_c and L_c, the (*10*) reflection—for measurement of L_a. The d_c dependence on HTT allows for allocating three areas: 1000–1500°C (d_c decreases from 0.347 down to 0.344 nm), 1500–2300°C (d_c is practically constant and makes 0.344 nm) and above 2300°C (d_c decreases and reaches 0.340 nm at 2800°C). These results contradict with the data described above [13]. It is noteworthy, that d_c of the soft forms of carbon depends on annealing temperature in a similar manner [27], thus, probably, indicating inhomogeneity of the GC material investigated [15]. The parameters L_a and L_c grow as HTT becomes higher. They vary more monotonously, than d_c, though the rate of increase elevates at temperatures above 2300°C. In the investigated interval of HTT L_a changes from 2.8 up to 5.0 nm, and L_c—from 1.0 up to 2.8 nm. Last two values correspond to an increase of the average number of layers in the stack from 3 to 8 in agreement with [13].

In works by Ergun [16] and Ergun and Schehl [17] a GC sample synthesized at 3000°C was investigated. Both the methods of Fourier analysis of (*110*) reflections and of the diffraction spectra reconstruction from a structural model were applied. The following features of the GC atomic lattice are established: completely resonant but distorted rings dominate in the structure; however there exist folds of the layers which produce strains in a lattice, hence quinoid rings are sited mostly close to folds. These results are in conformity with the conclusions concerning anisotropy of a tension distribution in the GC structure [13].

In one of the pioneer works Noda and Inagaki [18] on the basis of GC diffraction data have stated a hypothesis that tetrahedral (diamond-like) bonds connect the small areas of graphite-like layers between themselves. This model is denied, however, by the results of Mildner and Carpenter [23] and of Wignall and Pings [26] that show no significant amounts of tetrahedral bonds in GC.

Pesin and Serezhenko [19] have made an assumption that the energy excess of carbon layer borders [28] results in the size distribution of microcrystals and determines the character of this distribution. This excess manifests itself in the raised values of microcrystalline carbon enthalpy [27], and, on the other hand, competes with the thermal effect in the course of GC synthesis. The aim of the work [19] was reproducing the X-ray diffraction pattern shapes by taking into account the size distribution of carbon layers and determining the distribution type by comparing with experimental results.

Wide diffraction patterns of GC are convenient objects for the solving of this problem, as the instrumental broadening has a little influence on the shape of a wide line. Besides GC macroscopic structure is extremely isotropic, and that allows not taking into consideration the texture effects on the X-ray reflection intensity. The analysis of the angular dependence of the (*10*) and the (*110*) reflections width has shown, that the influence of interplane distances variations on widening of the patterns can be neglected in comparison with that of GC microcrystallinity.

Khachaturyan [29] has proposed an exponential model of crystallites size distribution based on general statistical considerations:

$$W = A\exp(-uL/kt) \tag{1}$$

Here W is the probability of a carbon layer with perimeter L existence, u is the exceeding energy of a unit of the perimeter of a layer length, k is the Boltzmann's constant, t is a characteristic temperature determined by the conditions of synthesis. The latter for the most of carbons can be identified as HTT. A is a normalizing constant equal to u/kt.

The Equation 1 corresponds to the known fact of a yield of large microcrystals increase with growth of HTT [27].

The yield of each reflecting layer in coherent scattering is represented by the Laue equation [30]:

$$I \sim \sin^2[(\pi xL/\lambda)\cos\theta]/\sin^2[(\pi xd/\lambda)\cos\theta],$$

where λ is the length of X-ray radiation wave; θ is the angle of maximum reflection (the angle of sliding, 38.8° for graphitic (*110*) reflection of Cu K_α radiation); d is an interplane distance (0.246 nm for graphitic (*110*) planes), x is the angular coordinate of a reflection profile point measured relatively to θ.

According to [31], small dimensions of layers results in shift Δ of the intensity maximum to the large angles direction. Its magnitude is inversely proportional to the size of a layer:

$$\Delta = \theta - \theta_0 = \frac{B}{L},$$

where $\theta_0 = 38.8°$, B is a coefficient of proportionality. Thus the contribution of a layer with perimeter L in the reflection intensity has a form:

$$I_L \sim \frac{\sin^2\{[\pi(x + B/L)\cdot L/\lambda]\cdot\cos(\theta_0 + B/L)\}}{\sin^2\{[\pi(x + B/L)\cdot d/\lambda]\cdot\cos(\theta_0 + B/L)\}} \tag{2}$$

In the specific case of the layers of equal size the symmetry of such a hypothetical polycrystal reflection shape follows from the Equation 2 symmetry.

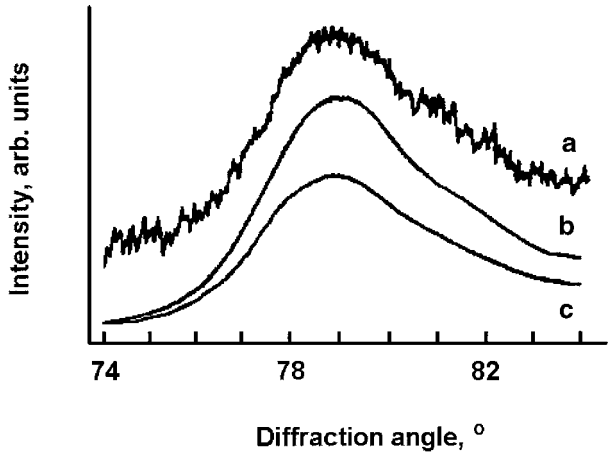

Figure 3 The steps of the (*110*) diffraction pattern treatment. Raw data for the GC sample heat treated at 2000°C are taken as an example.

Further taking into account the different probability of the existence of layers of various sizes, determined by the Equation 1, we come to the calculated angular distribution of the reflection intensity:

$$I = \left(\frac{u}{kt}\right) \int_d^\infty I_L \cdot \exp\left(-\frac{uL}{kt}\right) \cdot \mathrm{d}L \qquad (3)$$

The Equation 3 is a basis for computation in which the atomic scattering factor and the angular intensity factor [31] were taken into account.

For comparison with an experiment the diffraction spectra of four GC with HTT of 2000, 2500, 2700 and 3000°C (the samples 3–6, see Introduction) were investigated. They were obtained using copper radiation filtered by nickel ($\lambda = 0.154$ nm).

In Fig. 3 a sequence of the computer treatment of the experimental (*110*) pattern profile for the sample 3 is shown as an example. The initial curve (a) was smoothed out. Then a constant background was subtracted (b) in view of empirically found weak angular dependence of intensity of a background near to the (*110*) line. Finally the yield of the Cu $K_{\alpha 1}$ line was extracted out of the X-ray doublet (c). An asymmetry of the patterns shape is obvious for all the samples investigated. The increase of HTT shifts a reflection intensity maximum in the direction of smaller diffraction angles.

The fitting of the model and experimental pattern shapes was carried out for sample 3. This gave an opportunity to find parameters B and u (accordingly 0.07 nm and 0.115 eV/nm). Then keeping them constant and changing only parameter t according to annealing temperatures of other three samples, we have received the good consent of model and experimental shapes of (*110*) reflection. These results are shown in Fig. 4. The numberings of curves and samples coincide. It is readily visible that the model structures (dashed lines) are asymmetric and closely reflect the basic features of the experimental ones (solid lines). The increase of the parameter t results in the discussed above shift of a model reflection maximum to the smaller diffraction angles. Model intensity is underestimated in comparison with experimental one when the double sliding angle exceeds 79.5°. This divergence is noticeable for all four samples with a general tendency to increase with

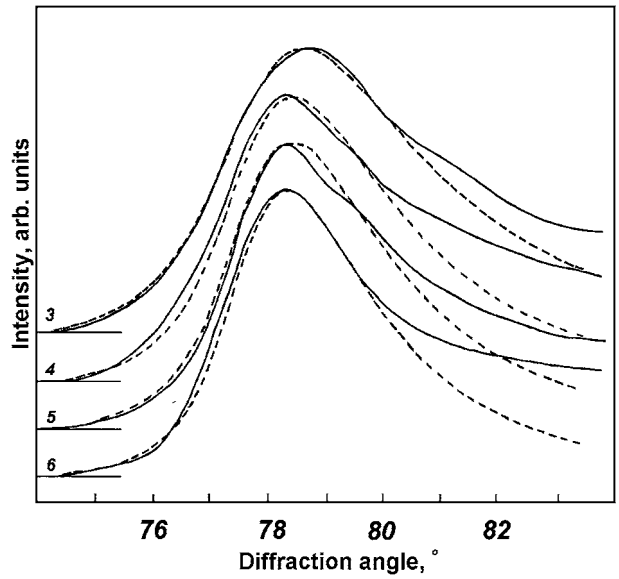

Figure 4 A comparison between the calculated (broken lines) and experimental (solid lines) (*110*) diffraction patterns.

growth of HTT. Apparently, this effect is connected with the presence in the GC diffraction spectrum of a weak (*112*) reflection, which maximum for graphite corresponds to 83.8°. The contribution of it increases with growth of HTT owing to the perfection of the GC crystalline structure, and thus distorts a shape of (*110*) pattern. But, according to curve 5 of Fig. 4 behaviour, this tendency is *not absolute* and thus some other explanations of the effect cannot be excluded. This fact itself gives a qualitative support for the assumption about non-monotonous modification of GC crystalline structure due to heat treatment.

The model also gives a reasonable quantitative agreement with experimental change of the maximum (*110*) reflection intensity of the samples 3–6. These results are given in Table I. Thus the conformity of experimental results to the model calculation confirms the existence of exponential size distribution of carbon layers in GC. As the edges of layers can act as traps of carriers, the knowledge of the distribution character is necessary for interpretation of not only diffraction data, but also of the results of electronic properties studies.

The additional data on a crystalline structure of samples 1–6 (HTT interval is 1200–3000°C, see Introduction) gives the analysis of (*002*) reflections. The analysis of (*004*) patterns of these samples is complicated. These reflections are displayed as separate inflow on a large angle side shoulder of (*10*) reflection only in diffraction spectra of samples 3–6. For samples 1 and 2 (*10*) and (*004*) patterns are visually indiscernible. The definition of an angular position of (*002*) (for sample 1) and (*004*) reflection maxima (for samples 3–6) can be

TABLE I The ratios of intensity maximum for calculated and experimental X-ray diffraction spectra of a sample 6 (I_6) to the appropriate values of all other investigated ones (I_0)

Sample number		3	4	5	6
t (K)		2300	2800	3000	3300
I_6/I_0	(Calculated)	2.14	1.41	1.29	1.00
I_6/I_0	(Experimental)	1,52	1.37	1.21	1.00

TABLE II Mean interlayer distances d_c in GC samples 1–6

Sample number	1	2	3	4	5	6
HTT (°C)	1200	1500	2000	2500	2700	3000
d_c, nm	~0.37	0.358	0.352	0.350	0.348	0.346

carried out only approximately because of significant width of the patterns. With increase of number of a sample the height of diffraction maxima elevates and their width diminishes, that testifies to the perfection of GC crystalline structure as HTT becomes higher.

The mean interlayer distances d_c for each sample was evaluated using angular positions of (*002*) maxima. These results are submitted in Table II.

From Table II data it is clear, that the increase of annealing temperature reduces d_c, and the results are in qualitative accordance with [13]: the reduction of d_c occurs more weakly if HTT becomes higher than 2000°C. Quantitative differences are connected, most likely, to distinctions of the raw materials used for the GC synthesis, which have different abilities to the structural development.

2.2. Other methods of structural analysis

Among electron microscopic researches of GC it is necessary to outline a basic series of works by Jenkins and Kawamura [see, for example, 1, 20], to which there is a huge amount of references for data interpretation. For instance, in [12] it is underlined that distribution of the lengths of two-dimensional domains, seen in microphotos [20], should correspond to the lengths of (l_0, L_0) rectangular chords, determined from X-ray diffraction data analysis. The sizes of the first are within the limits of 4–18 nm [20]. It should be noted, however, that only bottom limit is in the consent with the data of Rousseaux and Tchoubar [12]. The maximum value should correspond to a diagonal of this rectangular. Unfortunately the results in [12] give for a diagonal only about 11 nm that is essentially less than the anticipated magnitude.

The comparison of the experimental neutron diffraction data with the calculated spectra allowed Petrunin *et al*. [22] to attribute GC to a new class of materials—ultra dispersed bodies. The works on X-ray small angle diffraction enabled to define the character of porosity in GC. In [21] the research of pores form and sizes dependence versus both time of isothermal heat treatment and HTT was carried out (there were used the same samples, as in [15]). At constant temperature with increase of the annealing time the total volume of pores does not vary, but the specific area of their surface decreases. It means that isothermal treatment makes the pores merge. The increase of the pore volume with elevation of HTT is not a consequence of the light products of pyrolysis exit since a mass loss during heat treatment in the range 1000–2700°C does not exceed one percent. According to [21], the main sources of micropores formation are irreversible microcracks arising in GC owing to its anisotropic thermal expansion.

To similar conclusions lead the results of Wignall and Pings [26], devoted to the study of a GC sample heat treated at 1800°C. The pores of 0.8 nm are created due to the carbon ribbons shift relatively to each other along the basic planes. The sizes of a carbon matrix between the adjacent pores (1.6 nm) have appeared in reasonable conformity with the sizes of crystallites $L_a = 1.5$ nm, determined from wide-angle X-ray diffraction data. According to [26], the structure of the investigated material consists of micropores, formed by an infinite matrix of graphite-like laths. Wignall and Pings specify the physical meaning of parameters L_c and L_a for GC: L_c is an average distance between the pores, and L_a is that between the defects (folds).

3. Electric and magnetic properties

A wide number of GC physical properties are not defined by the character of interaction with electrical and magnetic fields of the whole system of carbon valence electrons. The large energy gap between the filled and free hybrid bands excludes direct influence of σ-states on such properties as electrical conductivity, thermoelectricity, Hall effect, magnetoresistance, magnetic susceptibility. As well as in other carbons with mainly graphite-like character of atomic arrangement, the major role in the listed phenomena belongs to highly mobile π-electrons, i.e. non-hybridized $2p$-states with poorly overlapping or touching valence and conduction bands.

The indirect influence of σ-states occurs due to creation of deep levels originated from the defects of crystalline structure. The localization of a part of π-electrons at these levels results in lowering the Fermi level below the point of π-bands contact [27].

The strong dependence of electrical and magnetic properties of graphite-like forms of carbon on the position of the Fermi level and the character of carriers scattering makes them sensitive to the peculiarities of crystalline structure. Thus, in addition to obvious technological importance, systematic studies of the effects of the annealing and measurement temperatures as well as of the magnitude and direction of external electrical and magnetic fields on electrical and magnetic properties allow us to make conclusions about a degree and a character of the atomic ordering in the studied form of carbon and to find distinctions of GC structure from other forms of graphite-like carbon.

3.1. The electrical conductivity

In 1966 Tsuzuku and Saito [32] investigated temperature dependence of the specific electrical resistance (SER) of a series of GC samples, obtained at various HTT between 800–3000°C. The increase of measurement temperature from 77 to 300 K monotonously reduces SER of all investigated samples. Annealing in an interval 800–2000°C reduces both SER value and a temperature coefficient of resistance. This effect is extremely considerable if HTT does not exceed 1300°C.

The results described in [32] are very interesting because of the unusual course of the SER temperature dependence for the sample heat-treated at 3000°C. At the ambient temperatures below 240 K its SER exceeds, but at higher temperatures becomes less than SER of the sample heat-treated at 2000°C. This fact we shall now keep in mind as the certificate of significant structural

transformations of GC in 2000–3000°C interval of annealing temperatures.

The experimental data of Kawamura, who has carried out SER study of GC in the measurement temperature interval 290–620 K were analysed by Hunt *et al.* in [33]. GC samples were heat treated in the interval 650–2700°C. The results have also shown, that both SER and its temperature coefficient decrease with the growth of annealing temperature. For interpretation the classical conductivity of semiconductors approach was used. Negative slope of temperature dependence of the resistance and its peculiarities were explained by the presence of energy gaps of two different origins, i.e. the "intrinsic" gap and the one caused by "impurities" or lattice defects. The latter decreases with elevation of HTT. The SER behaviour at low temperatures of measurement is ruled by the "impurity" character of conductivity, which exists due to the states formed by the defects and distortions of crystalline structure. The presence of an intrinsic gap is explained by graphite-like ribbon distortions. Therefore, SER magnitude and its temperature dependence character at high ambient temperatures have to depend largely on the ribbons size.

In [33] an attempt to change the width of the intrinsic band gap was undertaken by inducing of additional distortions of structure with static loading. The SER measurements were carried out at room temperature. The increase of the mechanical tensile stress actually elevated SER of the GC samples as the authors assumed with planning experiment. However, contrary to their forecasts, this effect was most pronounced at small annealing temperatures but almost disappears when HTT exceeds 1200°C. Piezoresistive effect reduction with the annealing temperature increase was explained by the Young modulus growth and decrease of the structure sensitivity to mechanical pressure. The results of measurements were reproduced with increase and reduction of loading. Effects of a hysteresis were not observed, that testifies to the elastic character of deformations and the absence of irreversible changes of the investigated sample structure.

In [34] GC samples obtained in the 1200–2700°C interval of annealing temperatures were investigated. The interval of measurement temperatures was 3–300 K. It was revealed that the GC specific electrical conductivity (SEC) is of the order 200 $\mathrm{Ohm}^{-1} \cdot \mathrm{cm}^{-1}$ and only weakly depends on the ambient temperature: the ratio of conductivity at 300 and 3 K makes from 1.12 up to 1.24 for the samples heat treated at different HTT.

In Fig. 5 the temperature dependence of SEC for GC samples with annealing temperatures 2550 and 1200°C (accordingly curves a and b) is taken from Baker and Bragg [34]. Unfortunately, in [34] no more result of the direct SEC measurements is submitted. However Fig. 5 shows that in all the investigated interval of ambient temperatures the conductivity of the first of the samples is less, than that of the second one. It very much reminds the behaviour of the samples with HTT = 3000 and 2000°C at low temperatures of measurement from [32]. Thus this unusual effect seems to be a common case for GC: the SER increase with elevation of GC HTT from 2000 to 3000°C was also reported by Yamaguchi [35].

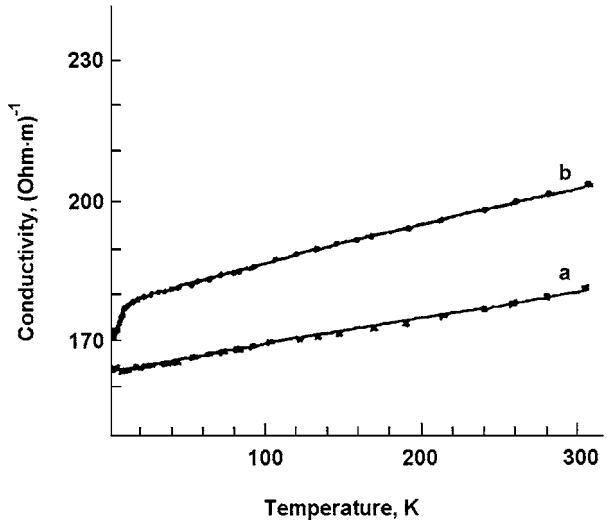

Figure 5 The electrical conductivity of two GC samples, having high (*a*) and low (*b*) heat treatment temperatures. The solid lines are calculated by the least square routine from the empirical Equation 4 (from [34]).

Baker and Bragg presented but in a narrower range of the ambient temperatures much more conductivity data in [36]. It was shown that GC SEC has a broad maximum around HTT ∼2000°C and corresponds well to the HTT dependence of the carriers number derived from the Hall coefficient measurements. The clear distinctions in conductivity and other parameters was revealed into HTT regimes above and below ∼2000°C.

An important feature that has been observed for the first time and specially outlined in [34] confirms the above conclusion: SEC of the GC samples, decreasing in general with temperature of measurement reduction, behaves in two various manners if annealing temperature is higher or below 2200°C. SEC temperature dependence of the samples with HTT above 2200°C at extremely low (∼15 K) temperatures forms a plateau with a weak minimum (Fig. 5, curve a). SEC of the samples with HTT lower than 2200°C considerably decreases with downturn of ambient temperature in an interval from 15 down to 3 K (Fig. 5, curve b). The last effect manifests the stronger the lower GC annealing temperature is.

The temperature dependence of SEC for all GC samples investigated in [34] follows to the empirical equation:

$$\sigma = A + B \exp[-(CT^{-0.25})] - DT^{-0.5} \qquad (4)$$

Here σ is the SEC, and T is a temperature of measurement. The curves with various parameters A, B and D well describe experimental results (solid lines in Fig. 5). The least square routine has allowed to define these empirical parameters for various GC samples.

The first and the largest of them (A) Baker and Bragg [34] attribute to a metal-band type of conductivity [37]. Its mean magnitude is about 176 $\mathrm{Ohm}^{-1} \cdot \mathrm{cm}^{-1}$ and does not depend on GC annealing temperature. The last fact is explained by small mean free path of carriers (∼1.3 nm). It is significantly less than the size of carbon layers in the researched HTT interval. Thus the growth of layers with annealing does not influence on

scattering of carriers character and, hence, on the value of parameter A. As a result, this parameter depends neither on HTT, nor on temperature of measurement [37].

The second term of the Equation 4 originates from Mott scattering with the hopping mechanism of conductivity. In most cases of this type of conductivity the drastic change of resistance caused by temperature dependence of the exponential term is observed. Therefore temperature dependence of parameter B is usually ignored. However, in GC case SER only poorly depends on temperature, so this approximation is not strictly proved. Nevertheless, as the various theoretical calculations predict opposite temperature behaviour of B, Baker and Bragg [34] considered this parameter as not dependent from temperature of measurement. In this approximation the parameters B and C have appeared identical within the error limits for all GC with various annealing temperatures. Hence, the whole second term in the Equation 4, connected with hopping conductivity does not depend on HTT. The power index of the temperature in the exponential argument indicates a three-dimensional character of carriers transport [34].

Essentially new result obtained in [34] is the existence of the last term, determined by one-dimensional conductivity and, hence, by the presence of one-dimensional conducting structures in GC [38]. This term gives the dominant yield at temperatures of measurement below 15 K. The parameter D (Equation 4) diminishes with increase of annealing temperature in the interval 1200–2200°C. At higher HTT it becomes extremely small. The nature of one-dimensional structures is not discussed in [34]. Baker and Bragg [34] proposed some hypotheses concerning the reasons of reduction of their yield to conductivity with increase of HTT: increase of their width and, accordingly, loss of one-dimensionality; reduction of their length; reduction of the mean free path of carriers. The effects of bonding of one-dimensional structures with each other and of their interaction owing to spatial affinity were not taken into account.

The important conclusion of [34] is establishing the fact of existence of one-dimensional fragments in GC structure alongside with graphite-like ones. The yield of the one-dimensional fragments decreases with increase of annealing temperature.

Such fragments may most possibly be carbyne-like carbon chains. With a rise of HTT the chains destroy owing to increase of ribbons width, thus changing the character of GC conductivity. The structural model of GC, including carbyne-like chains as elements of structure, could allow consistent explanation of Baker and Bragg's results [34]. This model will have further confirmation in the present review after the analysis of the emission properties of GC (Section 4).

3.2. The Hall effect and magnetoresistance

Yamaguchi [35], Baker and Bragg [34], and Tsuzuku and Saito [32] made the studies of GC Hall coefficient (HC). In [32, 35] the measurements were carried out at 20, 77 and 300 K; the maximum values of the magnetic field accordingly 1.35 and 2.2 T have been reached. In [34] interval of measurement temperatures was 3–300 K and maximum field was 5 T. In none of these studies the effect of magnetic field on HC value was observed.

The results of Tsuzuku and Saito [32] show the sensitivity of HC to GC heat treatment in the interval 1000–3000°C. At HTT = 1000°C HC is positive, at 1300 and 2000°C is negative, and at 3000°C again changes its sign. Its dependence on temperature of measurement has the following general character: the increase of measurement temperature reduces the absolute magnitude of HC irrespective of its sign, and the reduction is stronger the more HC absolute magnitude is.

On the contrary, Baker and Bragg [34] established, that HC of GC though depends essentially on the annealing temperature of a sample, practically does not depend on the ambient temperature. The results of this research are plotted in Fig. 6. Vertical bars attached to experimental points represent the limits of HC change for each sample in the whole interval of measurement temperatures. The data of Fig. 6 analysis show that the courses of HC versus HTT revealed in [34] and [32] are qualitatively similar to one another. However, the essential differences reflecting, apparently, the distinctions of structure and composition of precursory polymers in [34] and [32] are willingly seen. For example, the non-equal influence of measurement temperature on HC in these two studies is most likely the consequence of the various carriers' degeneration degree in GC samples, despite their nominally identical heat treatment. But the main distinction manifests in the HTT values, at which the sign of HC changes from negative to positive: in [34] this temperature makes about 1700°C, in [32] is more than 2000°C.

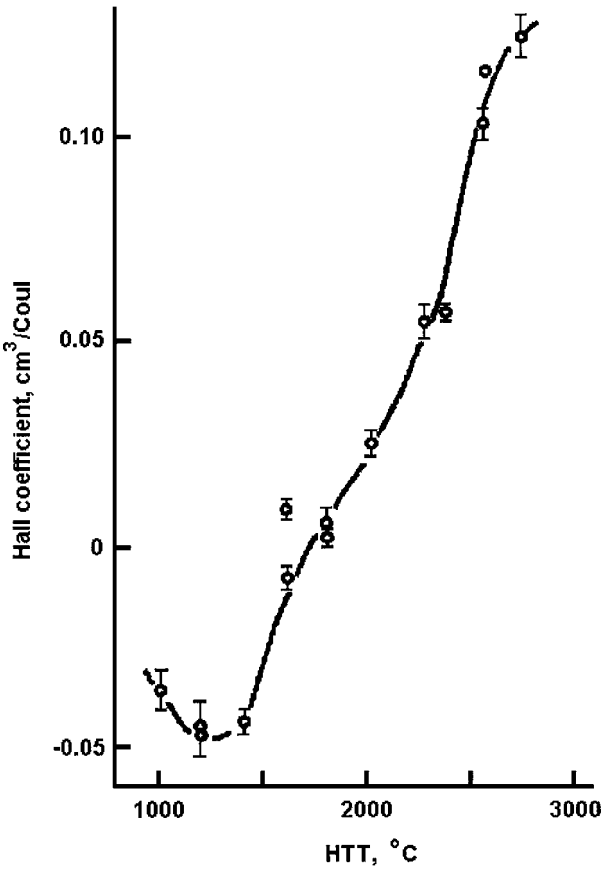

Figure 6 Hall coefficient of GC as a function of HTT (from [34]).

Yamaguchi [35] also observed a stronger HC dependence on the temperature of measurement than in [34]. At annealing temperatures smaller than 2600°C, the measurement at 300 K gave HC values exceeding the data at 20 and 77 K, but at HTT higher 2600°C the results were just opposite. A GC sample with HTT = 2600°C has identical magnitudes of HC at all three temperatures of measurement. The absolute values of HC measured in [35] are slightly less than obtained in [34], however their HTT variations in both papers are qualitatively rather similar: the inversion of HC sign occurs close to 1700°C.

It is specially outlined in [34], that the cumulative complex influence of many parameters of GC electronic structure does not allow not only to evaluate carriers concentration using a value and sign of the HC, but just a type of conductivity. The measurements of the Seebeck coefficient at room temperature [34] have shown its positive value for all the samples investigated, thus indicating that the major part of carriers were holes. This discrepancy of carrier signs determined from thermoelectricity and Hall effect data does not give an opportunity to interpret consistently the character of influence of structural transformations in the course of heat treatment on GC electronic structure.

Yamaguchi [35], Yoshida *et al*. [39], Saxena and Bragg [40], and Hishiyama *et al*. [41] have studied magnetoresistance (MR) of GC.

In [35] the interval of HTT was 900–3200°C. Time of isothermal heating at each maximum temperature was 15 minutes. The measurements were carried out at temperatures 20, 77 and 300 K. In the first case the holder with a sample was placed directly in liquid hydrogen, in the second one—in liquid nitrogen. The magnetic field reached 1.35 T. MR of the most of the investigated samples was negative, that is characteristic for defective graphite-like carbon bodies [27]. The exceptions were the samples heat treated at 900 and 1000°C, which MR at 20 K were weakly positive (accordingly ∼0.2 and 0.1%), and at other measurement temperatures are close to zero. A growth of annealing temperature as well as a reduction of measurement temperature gave rise to the absolute value of negative MR, which reaches 3.2% for the sample with HTT = 3200°C at 20 K.

The detailed MR studies in magnetic field up to 5 T and in 10–300 K interval of measurement temperatures of the GC samples heat treated between 1000 and 2800°C were carried out in [40]. It is revealed, that for all the investigated samples MR has a negative sign and increases in absolute value with growth both of HTT and of the magnetic field and with reduction of temperature of measurement. These results are in the qualitative consent with [35]. It was stated that in wide intervals of measurement temperatures and magnetic fields the value of negative MR is proportional to the ratio $B/(T^{0.5})$, if HTT exceeds 2000°C.

In [41] MR of the GC sample with HTT = 3000°C was measured. At 1 T and 77 K its MR was negative and made −0.03%, that is consistent with the data in [35, 40].

Comprehensive research of GC by scanning electronic microscopy, X-ray diffraction and the MR measurements were carried out in [39]. MR was measured at 77 K (a holder with a sample was immersed in liquid nitrogen). Two samples with the smallest annealing temperatures (∼1000°C) were investigated in magnetic fields up to 6.5 T using a superconducting electromagnet. Even in such giant fields the MR effect in these samples was not found. MR of GC samples with HTT = 2000 and 3000°C was negative and grew up as well as in [35, 40] with increase of HTT and magnetic field (up to 1 T), reaching ∼0.065% for the last sample in good conformity with the results of Yamaguchi [35].

TABLE III Mean values of grains (D) and coherent scattering domains (L_a) sizes

D (nm)	6.0	7.0	9.4	10.0	13.1
L_a (nm)	2.0	2.5	3.0	3.1	3.5

Source: Yoshida *et al*. [39].

The data of [39] have revealed correlation of the average sizes (D) of grains noticeable by electron microscopy on fractured surfaces of GC samples with the sizes of CSD along the crystallographic direction a (L_a). These results are displayed in Table III.

The analysis of the Table III data shows that the dependence found in [39] has monotonous non-linear character.

The important result of [39] is a conclusion about existence of the minimum size of graphite-like structure elements ($L_a = 2.7$ nm) necessary for negative MR survival in a sample.

3.3. The Seebeck effect

Tsuzuku and Saito [32], Hishiyama *et al*. [42], Yamaguchi [43] and Pesin [44] investigated thermoelectric properties of GC.

In [42] Seebeck coefficient (SC, α) was measured in 1.5–280 K interval of temperatures. The same GC samples, as in [34] (annealing between 1200 and 2700°C), were used. The empirical equation, describing the dependence α on measurement temperature was received:

$$\alpha = aT + b(T^{0.5}) + \alpha_B$$

The first and the second terms in this equation are connected, according to [42], with conductivity of a metal type and hopping conductivity correspondingly. The third term provides a sharp feature of the temperature dependence of α with a maximum about 23 K.

Not only the measurements of GC specific electrical resistance and Hall coefficient, already described in the previous sections, were the scope of work [32], but as well the study of its SC temperature dependence. These results have shown, that the SC of the samples having HTT = 800, 1000, 2000 and 3000°C grows with the increase of measurement temperature in 120–770 K interval. For GC heat treated at 1000 and 2000°C α changes a sign from negative to positive. Exception is the SC temperature dependence of a sample with HTT = 1300°C: its α is negative and poorly grows on absolute size with elevation of measurement temperature. The last fact testifies to the significant structural transformations in GC due to annealing at temperatures close to 1300°C that is in accordance with the data on specific electrical resistance. SC variations of GC samples at different temperatures with an increase of annealing temperatures up to

2000 and 3000°C indicates recovering of the structural defects manifesting as acceptors [27].

In [43] the thermoelectricity of the thermocouple composed of GC and polycrystalline graphite rods was studied. Annealing temperature of both materials was 3000°C. The length of the rods was 45 cm, and the diameter sized of 0.5 cm. The rods were put into contact and located in the centre of the cylindrical graphite furnace. The external ends of them were kept at room temperature. The temperature in a zone of contact was measured by optical pyrometer, and voltage of the thermocouple by potentiometer. The measurements were carried out in the temperature interval 1100–3300 K, but Yamaguchi [43] made an attempt to extrapolate the real experimental dependence to the interval 300–1100 K and found that at the measurement temperature of about 800 K α of GC, defined *relatively* to polycrystalline graphite, should have a maximum. Regretfully, Noto *et al*. [45] have used such an ambiguous result for data interpretation.

In [43] the data of SC measurements relatively to platinum for a series of GC samples heat-treated between 1100–3000°C are also presented. The measurements were carried out at room temperature. The SC magnitude monotonously grows the higher HTT is, that contradicts the data in [32] (probably, because of absence in a series of a sample with HTT close to 1300°C), but well corresponds to the results of Hall coefficient measurements made with the same samples [35].

Pesin [44] has studied the temperature dependence of SC for GC heat-treated between 2000 and 3000°C (samples 3–6, see Introduction). The natural temperature gradient created by a heating furnace was used. SC was measured relative to platinum. Absolute SC value was calculated at each temperature of measurement using tabulated values for platinum. The results showed that SC of these samples is positive and independent of the magnitude and direction of the temperature gradient in the entire temperature interval studied (300–1200 K). The measurements of each sample were carried out twice, and the results had good reproducibility (within the error limit of 3%). The pressure of air in the evacuated chamber did not exceed 1.5 Pa. Such moderate pumping has appeared sufficient to prevent sample oxidation. The temperature variation of α on heating reproduced that on cooling for each sample, testifying to absence of irreversible changes in the samples during this course of measurements.

These data are shown in Fig. 9. The enumeration of curves and samples coincide. The Figure shows a different behaviour of SC versus temperature plots for each sample. α of a sample 3 in the interval 300–820 K grows from 6.0 up to 14.7 μV/K, at the further heating up to 890 K practically does not vary, then again increases, passes through a wide maximum reaching 16.7 μV/K and slightly decreases above 1120 K. SC of a sample 4 in the interval 300–790 K grows from 7.2 up to 15.4 μV/K, in the interval 790–1010 K does not depend on temperature within the experimental error limits, then decreases down to 14.2 μV/K at 1170 K. α of a sample 5 increases from 7.9 up to 14.0 μV/K in the interval 300–670 K, at the further heating there is a tendency to weak growth up to 14.5 μV/K at 1170 K. α of a sample 6 depends on temperature quite similarly: in an interval 300–620 K it increases from 8.7 up to 13.0, and then poorly grows up to 13.5 μV/K at 1170 K. At temperature about 510 K temperature variations of SC of all the samples demonstrate a bend, which is stronger the higher is the annealing temperature of a sample.

There is one more peculiarity shown in Fig. 7 which is not inherent in soft forms of carbon [27], i.e. the intervals of ambient temperature in which α does not

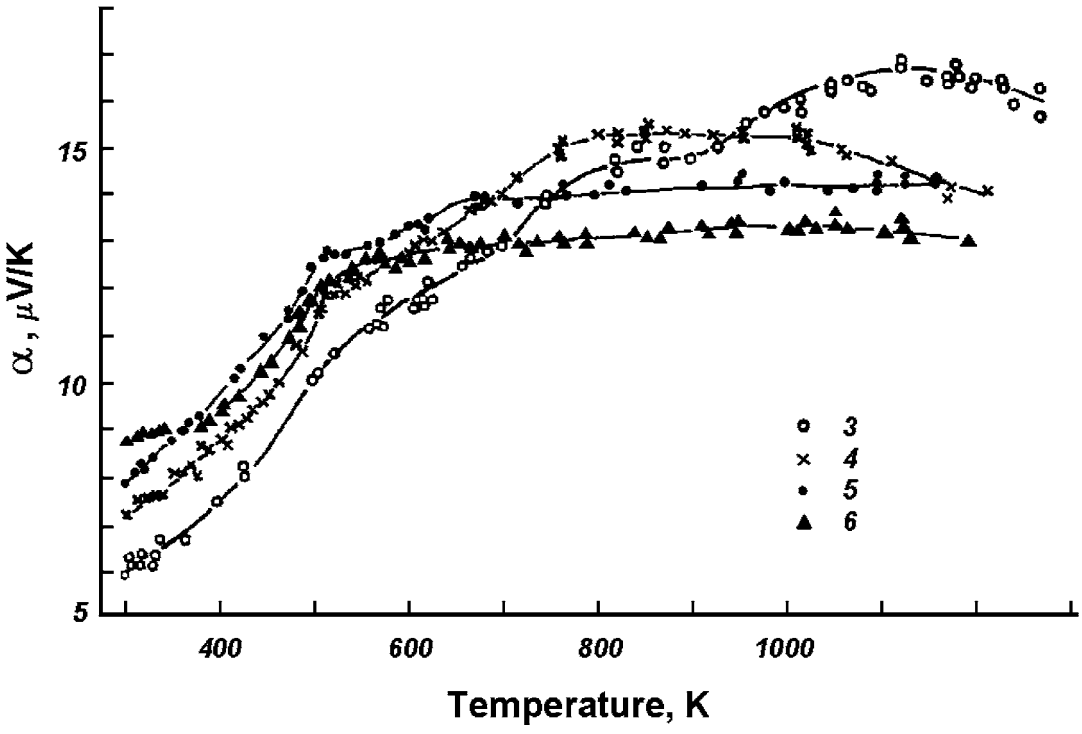

Figure 7 Seebeck coefficient variation of the GC samples heat treated at 2000, 2500 2700 and 3000°C (accordingly curves 3, 4–6) versus ambient temperature.

change or varies extremely weakly. The detection of this feature reveals a new experimental fact reflecting a specificity of GC electronic structure. For an interpretation of this result it is necessary to assume existence of "impurity" levels in GC conduction band. Their density should exceed that of free states of a two-dimensional carbon layer in the same energy range. Such capacious levels in a conduction band near to the Fermi energy have really been found in GC [46].

When ambient temperature is sufficiently low only a small number of electrons is activated in these levels, which act as acceptors. With increasing of ambient temperature the position of chemical potential moves to the top of the valence band and SC grows. At higher temperatures the localization of large number of electrons in "impurity" states results in the chemical potential diving into the valence band and stabilization of α. Filling of the acceptor levels by the carriers activated from the valence band and further activation of electrons in the conduction band due to temperature elevation promote the chemical potential displacement again to the valence band top and SC passes through a maximum, characteristic for graphitizable carbons [27]. This very case is realized in a sample 3. For sample 4 the temperature interval, in which there occurs a filling of the "impurity" levels by the carriers and α is constant is wider than for sample 3. It is apparently connected with the increased capacity of these levels due to GC HTT growth. In samples 5 and 6 the capacities are so great that the filling of the levels proceeds even at temperatures close to 1100–1200 K.

Reduction of the ambient temperature at which the filling of acceptor levels begins (the low-temperature edge of the plateau of α temperature dependence) with increasing HTT demonstrates the rapprochement of these levels to the Fermi energy. It is in accordance with the ideas about the influence of heat treatment on the Fermi energy of graphite-like carbon structures [27].

To check these qualitative assumptions the temperature dependence of chemical potential and SC was calculated. We used a two-dimensional model of graphite that differs from Haering-Wallace model [47] by the presence of an empty "impurity" energy band. Owing to qualitative character of calculation the density of state (DOS) energy dependence through this band was chosen in a simple and symmetric form:

$$G(E) = A \exp(-|E - E_0|/\sigma$$

Here A is maximum DOS of an "impurity" band; E is the energy of the charge carrier; E_0 is energy position of the DOS maximum; σ is a parameter of the bandwidth.

The result of the calculation of the chemical potential temperature dependence can be expressed by the following equation:

$$\varepsilon^2 = \varepsilon_0^2 - \frac{\pi^2}{3}(kT)^2 + 4(kT)^2 F_1\left(-\frac{\varepsilon}{kT}\right) + 2\frac{A}{B}\int_{-\infty}^{\infty} \frac{\exp(-|E - E_0|/\sigma)\,\mathrm{d}E}{\exp\left(\dfrac{\varepsilon - E}{kT}\right) + 1}$$

Here ε is the chemical potential value at temperature T; ε_0 is the Fermi energy; k is the Boltzmann constant, $F_1(-\varepsilon/\kappa T)$ is the Fermi integral of an unit index; $B = 53.4 \times 10^{20}$ eV^{-2}cm^{-3} is a band parameter of two-dimensional graphite [47]. The energy is measured in the direction of the valence band from a point of contact of π-electronic bands of two-dimensional graphite.

For the calculation of α we used the equation obtained for one type of carrier,

$$\alpha = \frac{\varepsilon}{eT} \exp\left(-\frac{\varepsilon}{kT}\right)$$

Here e is an electron charge. A positive sign of the SC experimental values justifies its use in the entire investigated temperature interval. This fact testifies to mainly hole-type yield to thermoelectricity.

The calculations of ε and α were made by an iterative way. The limits and step of integration were selected so that the result of computations did not depend on them. In Fig. 8 calculated $\alpha = f(T)$ variations qualitatively similar to the experimental ones are shown. This similarity has appeared possible only with a certain choice of "impurity" band parameters. The parameter A was adopted 13.35×10^{22} eV^{-1}·cm^{-3} and did not vary. The magnitudes of parameters ε_0, E_0 and σ and also the result of "impurity" atom concentration N calculation are listed in Table IV. A negative sign of the parameter E_0 corresponds to an "impurity" band DOS maximum position in the conduction band of two-dimensional graphite.

Comparison of Figs 7 and 8 and Table IV data show, that the increase of GC annealing temperature results in increasing concentration of "impurity" atoms, in broadening of the band formed by them, and its displacement on an energy scale. These facts are in accord with the band theory basics regarding energy band evolution due to reduction of the distance between the adjacent atoms.

The decrease of the Fermi energy ε_0 apparently characterizes the heat treatment influence on decreasing the content of interlayer defects acting as acceptors of π-electrons [27, 47].

Thus, an employment of a simple model taking into account an "impurity" band just above the Fermi level gives satisfactory explanation of the experimental data on GC thermoelectricity obtained in [44]. At first sight the enormous ($\sim 10^{22}$ cm^{-3}) content of "impurity" states leads to the assumption that their origin is connected with existence of the large number of edge atoms of narrow graphite-like layers. Edge atoms can exist in some peculiar energy states in comparison with the atoms inside a layer [28]. This assumption qualitatively proves to be true by Baker and Bragg [34, 38], who

TABLE IV Parameters of calculated $\alpha = f(T)$ curves 1–3 in Fig. 8

Curve number	ε_0 (eV)	E_0 (eV)	σ (eV)	N (10^{22}, cm^{-3})
1	0.16	0	0	0
2	0.11	−0.3	0.03	0.80
3	0.06	−0.25	0.05	1.34

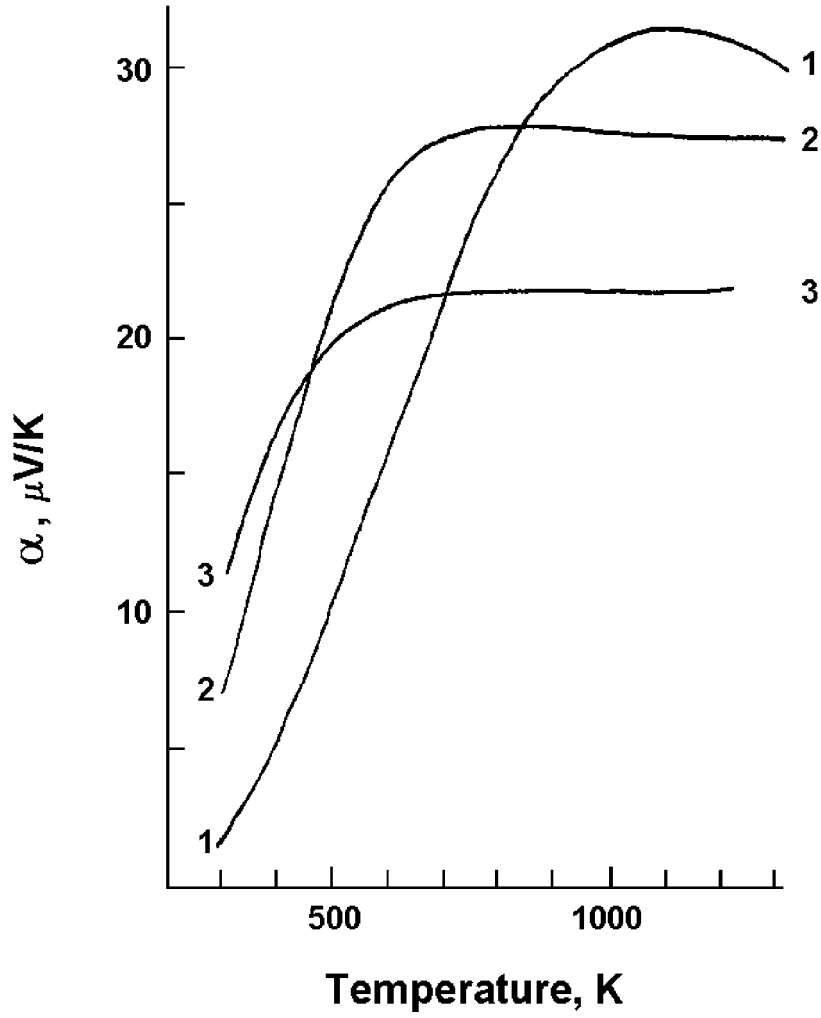

Figure 8 Calculated temperature variation of Seebeck coefficient for graphite-like carbon with an "impurity" band (all the parameters are listed in Table IV).

established the presence of one-dimensional structures in GC. However this does not correspond to the increase of "impurity" concentration when HTT rises. The growth of graphite-like sheet dimensions in the course of annealing is the fundamentally confirmed fact and it can result only in reduction of the edge atom yield.

The increase of acceptor level capacity in the conduction band with elevation of HTT between 2000–3000°C probably originates from the growth of the number of interstitial carbon atoms [48–51] as a result of structural reorganization of GC. The penetration of carbon atoms between graphite-like layers can be the cause of increase of the interlayer distance measured from an angular position of (*004*) diffraction pattern and observed in the same interval of annealing temperatures [13]. Moreover, creation of additional carrier scattering centres as a result of interstitial defects arising from such penetration can explain the increase of electrical resistance of GC samples at low measurement temperatures when annealing temperature becomes higher than 2000°C [32, 34, 35].

In conclusion it is necessary to note the fact of monotonous dependence of SC magnitude measured at room temperature on HTT of GC between 2000 and 3000°C [32, 42–44]. It has allowed Volga *et al*. [52] to propose a simple method of the indirect measurement of high temperatures with the help of SC room temperature values of GC samples "witnesses", which have undergone to the same thermal influence.

3.4. Magnetic susceptibility

Fischbach [14], Noto *et al*. [45], Fischbach and Rorabaugh [53], and Pesin [54] studied GC magnetic susceptibility (MS).

Fischbach [14] has investigated the variations of GC magnetic characteristics at room temperature due to the following factors: magnetic field in the interval of 0.6–1.6 T, annealing temperature in the interval 2000–3200°C and high-temperature deformation of samples. The semi-quantitative chemical spectral analysis has shown that the samples contain a number of impurities, which concentration is insignificant and, as a rule, decreases with increase of HTT. Among them there is iron, ferromagnetism of which results in MS field dependence. Employment of the standard Honda-Owen extrapolation technique allowed definition of the "true" MS (with a subtraction of iron MS) and also the concentration of iron. The last has appeared in reasonable conformity with the data of spectroscopic analysis.

The measurements of specific MS were carried out by the Faraday method at three mutually perpendicular orientations of samples respectively magnetic field. MS anisotropy was characterized by the ratio of maximum

among thus obtained three values to minimum one. The approximate size of samples was $3 \times 3 \times 3$ mm^3.

The non-deformed GC samples have appeared practically isotropic; the specified above ratio did not exceed 1.06. The deformation of GC samples at high temperatures (1600–2900°C) led to essential magnetic anisotropy of the originally isotropic material. The stretching deformation of 24% increased this ratio till 1.82, and the least MS value was reached in case of the magnetic field vector and a direction of a sample deformation coincidence. True MS (after a subtraction of iron impurity yield) of all the investigated samples was negative. Its dependence on the annealing temperature has appeared monotonous and almost linearly growing on absolute size. Diamagnetic susceptibility (DMS) values after averaging over three directions varied approximately from -3×10^{-6} up to -5.7×10^{-6} cm^3/g in the whole HTT range.

One of the most important results of [14] was an assumption about the structural model of GC. Four years before Jenkins and Kawamura [1], Fischbach, analysing the experimental data on GC X-ray diffraction and diamagnetism, marks [14]: "Bonding between the layer plane edges of crystallites would be expected too stronger than bonding between layer plane faces or between faces and edges. With a macroscopically random crystallite texture, this could have the effect of creating tangled chains of crystallites reminiscent in many ways of the structure of uncrystallized long chain polymers." Fischbach explains the anisotropy induced in the deformed samples by straightening of the chains in a direction of the applied mechanical stress.

To obtain information about parameters of GC π-band the temperature dependence of MS of several samples heat treated at 800, 1000, 1300, 2000 and 3000°C were studied in the range 77–300 K [45]. To check the presence of ferromagnetic impurity in the samples the field dependence of MS (up to 1 T) was also investigated. The last one was not revealed, that testified about neglecting small content of impurity. The measurements at room temperature have shown, that MS grows with increase of HTT not monotonously: there is a weak minimum at 1300°C. Noto *et al*. [45] explain this feature by the creation of large number of localized paramagnetic spin centres due to GC structural rearrangement near to this temperature. The similar effect is observed in graphitizable materials with annealing at temperatures close to 600–700°C.

The temperature variations of MS are analysed in [45] on the basis of two-dimensional graphite calculation [47]. Such analysis has allowed the determination of the Fermi energy in GC samples heat-treated at 2000 and 3000°C (accordingly 0.16 and 0.11 eV below the point of a contact of the almost filled and unoccupied π-bands). The last value is then compared to the Fermi energy estimated from the results obtained in [32, 43] taking into consideration the ambient temperature appropriate to a maximum of the Seebeck coefficient.

This estimation is, however, extremely doubtful. Indeed, in [32] the increase of α was observed up to temperatures close to 900 K, and in [43] rather approximate extrapolation gives recession of *relative* SC at temperatures exceeding 800 K. These data are obviously insufficient to convince in existence of the maximum α *absolute* value of a sample with HTT = 3000°C and just very at 900 K.

In [53] the measurements of magnetic properties of GC samples were carried out for study of ferromagnetic impurities evolution and as well for determination of effective kinetic activation energies of crystalline structure reorganization due to increase of temperature and time of heat treatment. To study the kinetics of structural modification the samples with different times of isothermal treatment at various HTT in the range 2400–3000°C were made. GC samples were previously placed in a zone of the furnace, where temperature was approximately 500°C less than that of a central uniformly heated zone. The furnace was heated with a speed ~100°C per a minute up to temperature of slightly above necessary value. Then the container with a sample was quickly replaced in the central zone. The samples reached the final temperature approximately in 30 seconds after moving. At the end of a desirable interval of time switching off the furnace quickly reduced the temperature.

MS was measured at room temperature by Faraday's method at magnetic field in range 0.45–0.70 T. Owing to GC isotropy the MS measurements were carried out only at a single orientation of a sample in magnetic field.

The measurements of the samples with identical isothermal treatment time have shown the amplification of MS field dependence in the interval 1000–1400°C of annealing temperatures. Further increase of HTT weakened MS field dependence, which completely disappeared at 1800°C. Such unusual MS behaviour Fischbach and Rorabaugh [53] explain by chemical transformations of iron-containing impurities during heat treatment.

An alternative explanation of the initial rise of MS field dependence could be based on the assumption of the replacement of iron atoms to the periphery of growing carbon crystallites, and, thus, the increase of iron atoms local concentration in the intercrystalline space. It leads to the amplification of the exchange interaction resulting in the impurity magnetic momentum increase.

As shown in [53], the true MS of GC (after a subtraction of the ferromagnetic contribution of an impurity) is negative and its absolute value rises monotonously in the 1000–3000°C range from -1.2 up to -5.2×10^{-6} cm^3/g, and near 1500°C a bend of this dependence is present.

The changes of MS depending on time of isothermal heating were analysed in [53] by superposition of the kinetic curves [11] with the assumption of the equivalent character of the annealing time and temperature influence on the processes of GC crystalline structure formation. This routine has allowed estimation of the effective activation energy of these processes (1500–1750 kJ/mole), that essentially exceeds the similar characteristic of the soft carbon forms (~1000 kJ/mole). A higher value of activation energy found in GC case is attributed in [53] to the microstructural stresses inherent in hard carbons. The crystalline structure development

initiated by heat treatment appears as consecutive breaks of several carbon-carbon bonds. Such rearrangement takes place due to the process of diffusion with atoms of introduction formation and thus activation energy is essentially large, than in case of diffusion by vacancies, characteristic for graphitizable carbon.

The analysis of the works [14, 45, 53] shows that MS of GC was investigated in a rather narrow temperature interval 77–300 K. In [55] there is only a short mention about MS measurements at low temperatures, however experimental results are not presented and, as the authors specify themselves, have only preliminary validity. Besides a large amount of data [27] shows that the DMS temperature variations for all non-doped graphite-like forms of carbon are well described by the universal equation proposed in 1955 by the famous French researchers of carbon A. Pacault and A. Marchand [56]:

$$K = K_0[1 - \exp(-T_0/T)].$$

Here K is diamagnetic anisotropy at temperature T, and its value is readily calculated from the experimentally measured average MS (χ) of a macroisotropic carbon body, K_0 is diamagnetic anisotropy at 0 K, T_0 is a temperature of electronic gas degeneration. The parameters K_0 and T_0 are determined by π-band structure and are individual for various graphite-like materials.

In this spirit an experimental check of Pacault-Marchand equation validity in case of GC is interesting. The magnitudes of its parameters could give important additional information about the features of GC energy band structure in comparison with other carbon solids.

To solve this problem four GC materials with HTT between 2000 and 3000°C (samples 3–6, see Introduction) were used [54]. The measurements were carried out at two values of magnetic field (0.4 and 1.1 T) by Faraday's method. In the whole interval of ambient temperatures (4–700 K) no field dependence of susceptibility was observed. All the investigated samples were diamagnetic. Measurements in 4–280 K interval were carried out using current balance MGD312FG. The technique of high-temperature measurements is described in [57].

The experimental results are displayed in Fig. 9. The numbering of points series forming experimental temperature variations of χ for each sample corresponds to the numbering of the samples. It is clearly noticeable

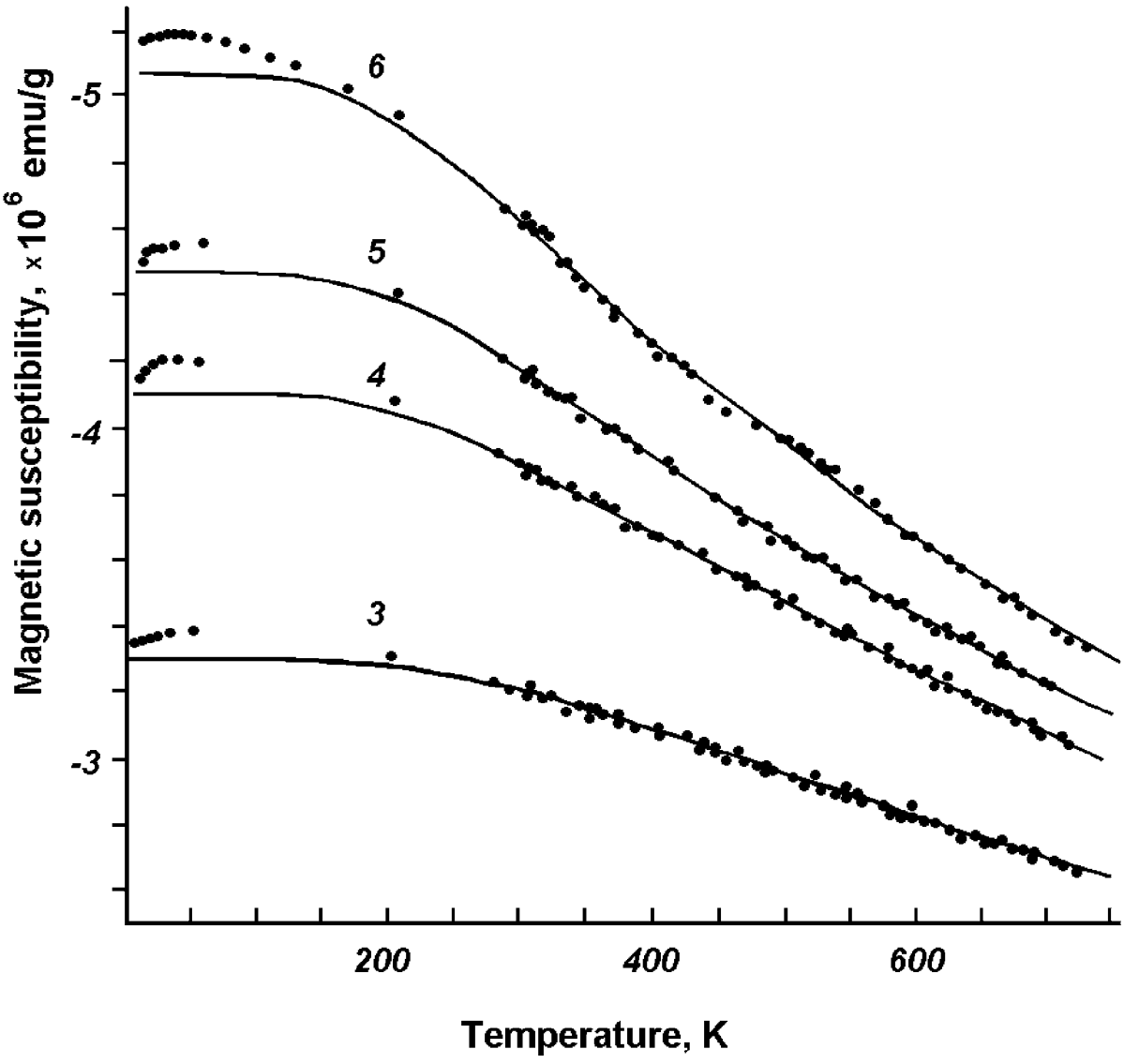

Figure 9 Magnetic susceptibility of the GC samples heat treated at 2000, 2500 2700 and 3000°C (accordingly curves 3, 4–6) versus ambient temperature.

TABLE V Best-fit Pacault-Marchand parameters for the 280–700 K DMS data [54]

Sample number	Annealing temperature, (°C)	K_0 (10^{-6} emu/g)	T_0 (K)
3	2000	7.35	990
4	2500	9.75	820
5	2700	10.85	750
6	3000	12.65	660

that DMS grows monotonously with increase of annealing temperature. This fact agrees well with the data reported [14, 45, 53]. Between 20–50 K all the investigated samples exhibit MS maxima. Reduction of DMS with downturn of temperature near to 40 K was found also in [55].

In the temperature range 280–700 K the experimental data obtained in [54] match well to the Pacault-Marchand equation and the parameters K_0 and T_0 may be determined for each sample. The results are given in Table V.

One can see that the increase of GC annealing temperature results in monotonous increase of K_0 and reduction of T_0. A similar influence of heat treatment on these parameters has been observed for other graphite-like forms of carbon earlier [27, 56].

The solid lines in Fig. 9 represent the calculated magnitudes of DMS obtained by substitution of the Table V K_0 and T_0 values in the Pacault and Marchand equation. It is clearly seen from Fig. 9, that at low temperatures of measurement (4–200 K) experimental DMS values for each sample exceed the calculated ones. The maximum difference between them, however, is not very significant ($<3\%$).

The DMS maximum at 20–50 K can be caused by low temperature amplification of the contribution of the localized paramagnetic centres, found in GC [55]. A similar maximum was observed also in DMS temperature dependence of graphite, but the interpretation given was related to the features of electronic structure [58].

According to various theoretical DMS calculation of two-dimensional carbon (see, for example, [47] and references therein) the value of K_0 is inversely proportional, and T_0 is directly proportional to the Fermi energy. Thus, the product of these parameters should be constant for all two-dimensional (or turbostratic [27]) forms of carbon. However for GC samples investigated in [54] the magnitude of this product grows with increase of annealing temperature.

It is known [45], that graphite-like carbons display temperature dependent electronic diamagnetism only if carbon layer length exceeds some critical size (∼3-5 nm). High-temperature annealing results in growth of layers; therefore there is an increase of the yield of these sufficiently large layers due to heat treatment. That provides an additional DMS growth and can be a reason for the effect found out in [54]. The last conclusion has a general character and can be confirmed by the analysis of the numerous data on DMS temperature variations of other forms of turbostratic carbon (see, for example [27, 56] and references therein).

4. Spectroscopic methods

The important information on the chemical composition and the energy state of a surface of solids is provided by widely used methods of optical, X-ray and electron spectroscopy. The variety of exact and complete enough calculations of the various forms of the condensed carbon energy band structure stimulates application of these experimental techniques to the study of carbon. They allow receiving the complementary items of information on a researched carbon object.

For example, the features of Raman spectra are determined by the energy dispersion of phonon states. The photoelectron spectra with X-ray excitation (XPS) reflect basically partial density of the filled s-type states, and the Auger electronic spectra (XAES) and soft X-ray emission spectra (SXS) are more sensitive to the valence electronic states of p-symmetry. The inverse photoemission spectra give the opportunity to receive reliable experimental information on density of empty states in the conduction band.

Below we shall describe the results of application of these methods to GC study. The physical processes upon which these spectroscopic methods are based are properly considered in special literature and their discussion is not a scope of the present review.

4.1. Raman spectroscopy

The Raman spectra of graphite-like carbon arise due to inelastic interaction of falling photons with the in-plane vibration modes of hexagonal layers within the depth less than 100 nm under a surface.

The researches and interpretations of Raman features in GC are carried out in a number of works [59–63]. The existence of two basic Raman bands at 1580 and 1360 cm^{-1} is revealed. The first of them is usually called as a "graphitic" (G-line). The second is not found in crystalline graphite and exists only in the defective carbons [59, 63]. It is close to the dominant Raman band of diamond (1332 cm^{-1}), but has received the name of a D-line not from "diamond", but from "disordered".

In Fig. 10 the Raman spectra of GC obtained by Nakamizo [59] (a) and Vidano and Fischbach [60] (b) are presented. From Fig. 10a the increase of intensity and narrowing of the D-band with increase of annealing temperature are well appreciable, while the G-band remains practically unchanged. The results reported in [60] (Fig. 10b) only partially correspond to the data in [59]: the D-band also is narrowed mainly from the side of the large wave number. The width of it decreases from 150 to 80 cm^{-1} with annealing of GC in the interval 1000–2600°C. Though the data on the D-band intensity changes as a result of annealing are not available from [60], however in comparison with the G-band intensity the data of Fig. 10b allow to notice non-monotonous changes with the general tendency to reduction that contradicts the results of [59]. Besides, according to [60], the most essential changes occur in the G-band, the form of which is rather complex due to its doublet character. Probably, these contradictions are connected with the distinctions of the samples synthesis conditions.

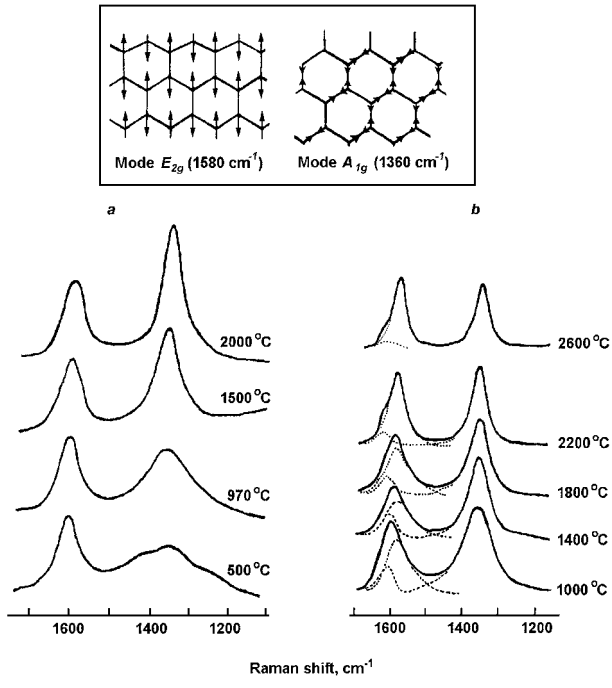

Figure 10 Raman spectra of GC (from [58, 59]).

It was stated in [60] that the G-band in GC can always be presented as a superposition of two components: G (1580) and D′ (∼1620 cm^{-1}). These are shown as shaped lines in Fig. 10b; and it is clearly seen that the elevation of annealing temperature causes in the decrease of the last component intensity. Though the nature of D′-line is not clear [60], its evolution with GC annealing allows to explain the "violet shift" of G-band in strongly disordered carbons.

The reason of Raman dispersion at 1360 and 1580 cm^{-1} is the excitation of the in plane vibrations A_{1g} and E_{2g} (see an inset in Fig. 10). E_{2g}-mode appears as the G-band and arises in all graphite-like structures. A_{1g}-mode is not excited in an infinite graphite crystal with hexagonal symmetry owing to selection rules, connected with the momentum conservation during phonons excitation. However this mode becomes active if the symmetry of a lattice differs from that of the hexagonal one due to structural defects, such, for example, as in GC with their small crystallites. This elucidates a high sensitivity of a D-band to structural ordering in carbons [59, 63].

Fitzer and Rozploch [61] have proposed the alternative explanation of the D-band nature and of the G-band "violet shift" in the disordered structures. On the basis of a simple idea about the length of internuclear bonds it was assumed that the vibrations of sp^3-hybridized atoms at the edges of graphite-like layers form a D-band in the disordered carbon structures. Such type of hybridization can arise, for example, in the region of contact of two layers located in crossed planes. This band suffers "a violet shift" in comparison with a D-band in real diamond having ideal sp^3-orbitals because of the fact, that the distances between carbon atoms in defective units are longer than that in graphite (0.1415 nm), but are significantly less than in diamond (0.154 nm).

This approach does not contradict to the results of the numerous researches, which have proved the absence of diamond-like regions in GC, as is based not on the analysis of a hybridization type, but on the estimations of internuclear distances. Besides the arrangement of carbon atoms with sp^3-hybridization of valence electrons primarily on the crystallites periphery excludes the formation of a compact phase with diamond-like atomic ordering.

If the peripheral atoms of a layer conserve sp^2-mode of hybridization, the distances between them will be less, than in graphite. That explains the G-band "violet shift" in carbons having the small sizes of layers. Such treatment also allows explanation of the results obtained in [60]. In case of the small sizes of layers the yield of the edged atoms is great thus resulting in high intensity of a D′-line, the nature of which is E_{2g}-excitation of peripheral atoms with the interatomic bonds shorter than in the central region of a layer. With GC annealing and growth of layers the yield of these atoms decreases. Accordingly, the D′-band intensity decreases.

In [62] the intensity and frequency of Raman bands for two GC samples with annealing temperatures 1800 and 2400°C with variation of primary photon energy and temperature of measurement in the range 90–310 K were studied. It has been revealed, that neither frequency, nor intensity within the limits of an experimental error does not depend on ambient temperature. The defects of crystal structure result in insignificant shift of bands but broaden them essentially. The G- and D′-bands have appeared to be tolerant to frequency of excitation, contrary to the behaviour of a D-band and weak lines G_1, G_2, D″ (the last three features are harmonics of the basic lines and occur accordingly at 2695, 2735 and 2950 cm^{-1}). The ratio of the D- and G-bands intensities grew with the reduction of excitation frequency, that testifies to the contribution of the resonant phenomena to the processes of Raman scattering of light by carbon structures [62].

In [63] the effect of density growth of GC heat-treated at 2500°C under action of a flow of xenon ions with the energy of 320 keV was studied by McCulloch *et al.* The earlier works of the same authors have shown that such processing raises the mechanical characteristics of GC. It makes possible to consider GC modified by ion bombardment as technologically prospective constructional materials. This comprehensive investigation of the ion irradiation doze influence included Raman spectroscopy, electron energy losses spectroscopy (in energy ranges both near to elastic peak and including ionization losses) and transmission electronic microscopy. The results obtained have allowed to develop a technique of the sp^3-hybridized electronic states yield measurement in the ion bombarded GC. In the pristine GC these states were not revealed in the consent with the results of numerous structural researches. Unfortunately, this technique can hardly to be considered as universal one due to the practical impossibility to separate correctly sp^3- and A_{1g}-mode yields in Raman spectra, especially if HTT is low.

4.2. Electron and photon spectroscopy

GC is a common object for the researches using XPS and SXS techniques (see, for example, [64, 65]).

However the study of electronic states of a *series* of GC samples, distinguished by the character of ordering of structure only due to different steps of heat treatment, is of special interest. The features of GC atomic structure, caused by the defects of various types, promote the formation of carbon - carbon bonds with the valence electron hybridization mode different from sp^2. The character and the quantity of the defects vary due to heat treatment and that should result in a manner of atomic wave functions superposition. These changes can be noticed by XPS, SXS and X-ray excited Auger electron spectroscopy (XAES) of carbon because of the well-known pronounced sensitivity of these methods to the symmetry of the initial state wave function.

An attempt to solve this problem in [64] was not fully successful owing to low resolution of the microanalyzer used. Besides selective sensitivity of each of the methods to *s*- and *p*-valence electron symmetry makes the results of GC study using only one of them very poor. Only comparison of experimental data received by different methods enables to reveal the changes of *s*- and *p*-electrons hybridization character by thorough comparison of the changes in relative intensity of spectral maxima reflecting the corresponding features of DOS.

Pesin and co-workers [66–68], and Kurmaev *et al.* [69] carried out such a cycle of researches. In [66, 69] valence electron XPS and SXS, in [67] XAES and in [68] core electrons XPS have been investigated (in all cases the samples of GC described in Introduction were used). A "working" surface of the samples was obtained by thorough preliminary mechanical scratching with a diamond scraper.

4.2.1. Experimental techniques

Photoelectron and Auger spectra of carbon were scanned using the magnetic electron spectrometer ES IFM-4 [70]. They were excited by non-monochromatic aluminium K_α- radiation filtered by an aluminium foil ($h\nu = 1486.6$ eV). The pump system provided oil-free vacuum with pressure of residual gases not exceeding 10^{-7} Pa.

The valence electron XPS and XAES were obtained in the intervals of binding energy accordingly 0–35 and 1173–1248 eV with passing energy of the analyser 300 eV (resolution about 3 eV). The core electron XPS were registered in the binding energy interval 280–319 eV with passing energy 100 eV (resolution ~1.5 eV).

For SXS measurement of carbons the vacuum system of soft X-ray spectrometer RSM-500 was specially modified [69]. It has allowed to reduce considerably a level of pollution of a surface of samples by hydrocarbons from residual gases. The test spectra of graphite and diamond obtained at pressure of the order 10^{-4} Pa are in good agreement with the results previously described in literature, which have been recorded under conditions of ultrahigh vacuum. A diffraction grid had a radius of 6 m and a period of 1/600 mm and provided the resolution not worse than 0.4 eV. All SXS measurements were carried out by E. Z. Kurmaev and S. N. Shamin.

4.2.2. Valence band spectra fine structure

In [66] the treatment of the raw valence electron XPS [66] and SXS [69] was carried out to subtract experimental noise and outline the really existing spectral features. The routine included standard procedures of smoothing [71] and instrumental broadening correction [72]. The treatment was fulfilled for all the spectra in a unique way, however intervals of smoothing were taken in conformity to different resolution of ES IFM-4 and RSM-500 spectrometers. The results are shown in Figs 11 and 12.

In Fig. 11 valence electron XPS of samples 3, 4 and 6 (see Introduction) are presented. The curve numbers correspond to numbering of samples. From Fig. 11 the satisfactory accordance of the basic maxima and inflows (*a*–*n*) energy position in the spectra of various GC samples is noticeable. The comparison with the previously published data [48, 65, 73] convinces, that the spectra shape is in general quite similar to that of graphite.

The survey spectra have shown the presence of oxygen on a surface of all the samples investigated the

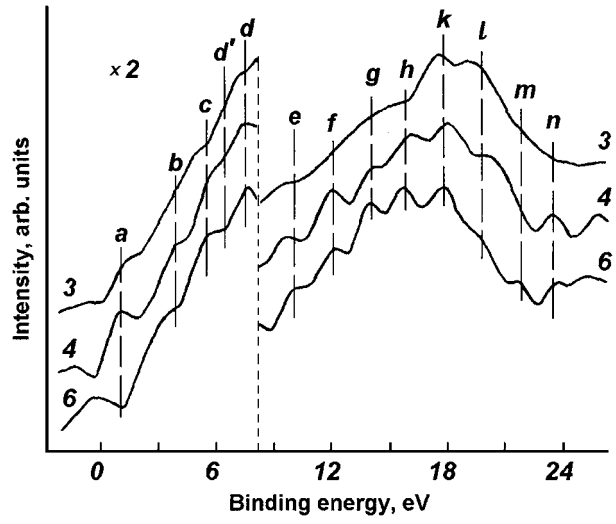

Figure 11 Valence band XPS of the GC samples heat treated at 2000, 2500 and 3000°C (accordingly curves 3, 4, 6).

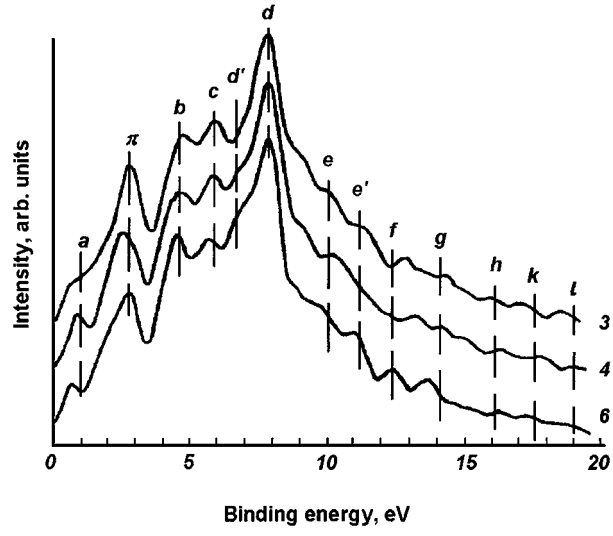

Figure 12 Soft X-ray CK_α-emission spectra of the GC samples heat treated at 2000, 2500 and 3000°C (accordingly curves 3, 4, 6).

amount of which decreases with increase of HTT. Oxygen influences the spectra shape: the O2*s*-states give appreciable inflow in GC spectra at binding energies close to 26 eV (Fig. 11).

It is clearly seen that the thermal annealing results in appreciable changes of valence XPS fine structure. Among them are the reduction of intensity of feature *l* and increase of intensity of features *f*, *g*, *h* and *n*. It is noteworthy, that the feature, observed at binding energies close to Fermi energy (*a*), is displayed only in XPS of GC and is absent in graphite spectrum. In spectra of samples 4 and 6 the features at binding energies about 12 (*f*), 16 (*h*) and 24 eV (*n*) are seen, which also are absent in a spectrum of graphite. Though the last one is situated close to O2*s*-feature, the spectrometer resolution is enough so that not to confuse them.

In Fig. 12 SXS of GC samples 3, 4 and 6 (see Introduction) are displayed. Photon energy 285 eV is accepted as zero of binding energy scale. The comparison with [48, 74, 75] also shows rather close similarity of the general shape of GC spectra to graphite spectrum. There is, however, an inflow at binding energy about 1 eV (*a*), which is absent in graphite.

The increase of GC HTT results also in changes of a relative intensity and shape of maxima π and *b* (Fig. 12). The first of them corresponds to the non-hybridized p_{z^-} electrons DOS maximum [48, 75]. Heat treatment increases the intensity of inflow d' (~6.5 eV). The spectra in Fig. 12 also contain a small maxima e' (~11 eV), which, as well as the maxima π, are not observed in valence XPS because of low sensitivity of the method to these electronic states.

The comparison of Figs 11 and 12 shows satisfactory conformity of energy position of the basic XPS and SXS fine structure features. Heat treatment changes intensity of some maxima. At binding energies exceeding 13 eV these variations are identical in both types of spectra. For example, intensity of a maximum *g* (~14 eV) grows with rising of number of a sample (or equally annealing temperature) in both figures. On the contrary, the intensity of inflow *l* (~19 eV) decreases both in XPS (Fig. 11) and in SXS (Fig. 12) due to annealing temperature of GC samples increase.

At binding energy smaller than 13 eV the valence states are formed mostly by hybridized electrons [48]. Therefore similar features XPS and SXS intensity variations during GC heat treatment reflect a process of redistribution of *s*- and *p*-states yield in hybrid bonds, or, in other words, a hybridization mode evolution of electrons having the appropriate energy. Thus it is not necessary to identify this phenomenon with spasmodic transformation of a coordination environment of carbon atom. Most likely a gradual change of a character of the defects in GC with heat treatment results in a rather smooth variation of a type of the hybrid wave function and, consequently, of the spatial distribution of electronic density.

In Fig. 11 in increased scale are presented XPS of GC samples investigated in [66] in a binding energy interval up to 8 eV. From this figure it is visible that the basic changes of the XPS shape as a result of annealing occur close to 1, 4.5 and 6.5 eV, that is at the same energy values, at which there are most essential SXS variations (spectral features *a*, *b* and d'; Fig. 12). With the elevation of GC annealing temperature the increase of the inflow d' in SXS is accompanied by the appearance and deepening of the hollow d' in XPS (Fig. 11). Such change corresponds to the amplification of *p*-character of electronic states with binding energy of ~6.5 eV. The further comparative analysis of Figs 12 and 11 shows the irregular variations of structure *b* intensity in SXS also accompanying opposite changes in XPS. Analysing changes of the feature *a* it is possible to make a conclusion that the heat treatment simultaneously moves it to the Fermi energy and reduces its intensity.

Those features of GC spectra, which are not specific for graphite, naturally cause the greatest interest. They reflect peculiarities of GC valence DOS, determined in turn by the differences of atomic arrangement in GC lattice from crystalline structure of graphite. The carried out experimental and theoretical researches of our own and the analysis of literature [19, 45, 48, 50] allow to propose a number of the assumptions about these features nature.

The feature *a* appears, apparently, due to the special energy condition of the carbon layer edges. Electrons of boundary atoms form their own energy band, which gets in the region of the interlayer electrons energy spectrum, forming resonant structure *a*. Due to heat treatment the sizes of carbon layers are increased [19, 45]. It results in reduction of relative number of boundary carbon atoms. This effect should reduce density of states in this band thus causing its narrowing and energy shift. This shift occurs in a direction of the Fermi level, where interlayer atoms DOS is small [47, 48]. Therefore boundary electrons states increase the total DOS near to the Fermi level. This change reveals in spectra as the inflow *a*. The presence of this feature both in XPS and in SXS of GC leads to a conclusion about hybrid character of boundary atoms electronic states. The above hypothesis explains the absence of a similar maximum in spectra of monocrystalline graphite, in which the carbon layers have a large diameter and consequently small relative number of boundary atoms.

In [48] the influence of interstitial (introduced between graphite-like layers) carbon atoms on the DOS of graphite is calculated. These data are displayed in Fig. 13. The curves correspond to DOS of the ideal lattice (a) and at presence of interstitials (b). The comparison of spectra from Figs 11 and 12 with the curves in Fig. 13 convinces that with GC annealing the probability of an attachment of out-of-layer atoms of carbon to growing carbon layers increases. It explains the reduction of the feature π and the increase of the inflow d' in SXS, and also occurrence of a maximum *n* (~24 eV) in XPS with increase of annealing temperature. Moreover, out-of-layer atoms give the valuable contribution to DOS close to spectral feature *a*, and this fact can enrich the above interpretation of this feature.

4.2.3. Auger spectra

In [67] XAES was chosen as a method sensitive to the features of DOS distribution along the valence band. It is known that the various types of carbon bonds,

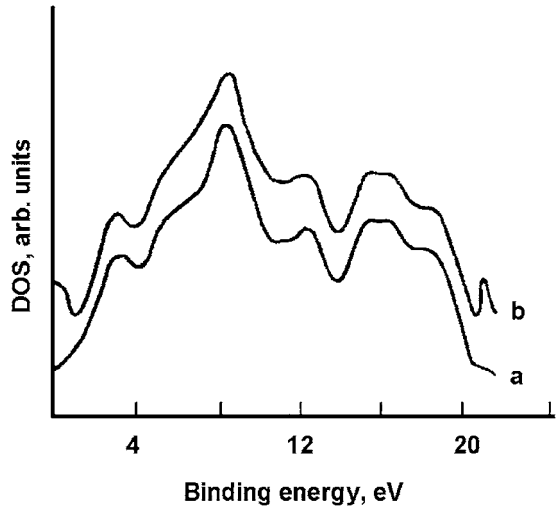

Figure 13 Calculated DOS of ideal (a) and intercalated by carbon atoms (b) graphites (from [48]).

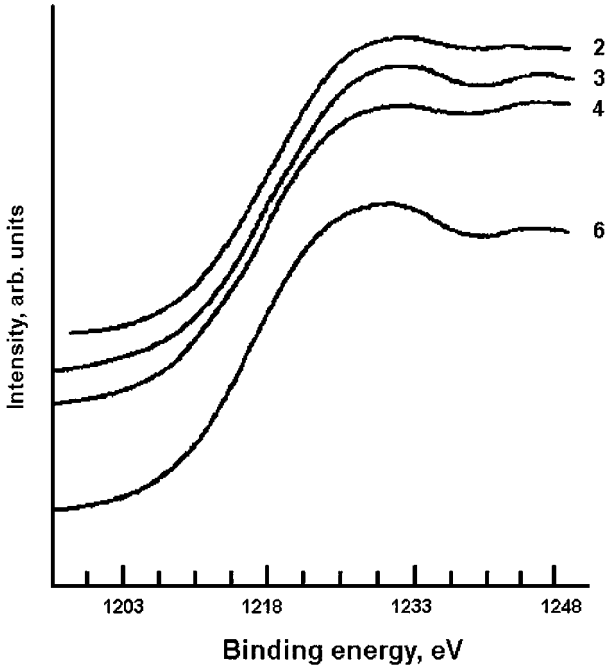

Figure 14 XAES of GC samples heat treated at 1500, 2000, 2500 and 3000°C (accordingly curves 2, 3, 4, 6).

distinguished by the hybridization character of valence electrons in *s*- and *p*-states, effect the shape and energy position of XAES [76–80].

To make the comparison with the results of other spectroscopic researches, for example with SXS, the simplified technique of experimental XAES self-unfolding (deconvolution) described in [76] was used.

In Fig. 14 the smoothed XAES of samples 2–4, 6 (see Introduction) are placed. The numberings of curves and samples, as well as in a number of the previous figures, coincide. The smoothing was carried out with the filter of width 3.7 eV, which a little bit exceeds the resolution limit of the spectrometer (the passing energy of 300 eV was used). From Fig. 14 it is clearly seen that XAES of all the samples investigated contains two basic features: actually C*KVV*-peak (1200–1237 eV) and a less intensive maximum at higher binding energy region (satellite). The origin of the last maximum has been investigated quite insufficiently yet. According to [77], it has a multiple nature, as is caused by characteristic shake-up of valence system by core and valence holes. In [78] an occurrence of this spectral feature is attributed to the plasmon excitation during delocalization of two valence holes in a final state of Auger relaxation. In [81] there was revealed, that the essential yield to the satellite intensity came from C*1s*-electrons exited by O K_a-radiation of oxides on a surface of the X-ray source anode in case of XAES generation by non-monochromatic radiation. At last, we cannot exclude an opportunity that this feature is a satellite of multiple ionization of an atom. It is connected with the Auger relaxation process in those of carbon atoms, which has lost during C*1s*-level photoionization one of the valence electrons as well, for example, due to shake-off process. Connection of the satellite with the main Auger-process can be also proved by the fact that its shape and intensity depend on a type of a crystal structure of carbon [82].

XAES treatment consisted of two steps. At first nonlinear subtraction of a background [71] from the spectra shown in Fig. 16 was made. Then their deconvolution [76] was carried out. This treatment of spectra of all the samples was done in a unique way. The obtained self-unfolded XAES are displayed in Fig. 15. The numberings of curves and samples coincide. All the spectra, except that of sample 6, are attached to a unique energy scale by the position of the main maximum. Such attachment has ensured satisfactory accordance of other features energy positions. Some repeating features are allocated with vertical broken lines (*a*–*e*). The feature π designates spectral peaks reflecting the main maximum of the p_z-electrons DOS (binding energy is about 2.5 eV).

The comparison of the data in Figs 12 and 15 shows, that SXS and self-unfolded XAES of GC have many similar features. They contain the same maxima; the intensity of self-unfolded XAES, as well as SXS, is high in the binding energy range 0–14 eV; the increase of GC annealing temperature elevates the maxima *b* and d' intensity in the spectra of both types. These facts testify that they really reflect the identical features of *p*-type valence DOS.

The detailed comparative analysis of Figs 12 and 15 also allows to reveal the difference between the spectra discussed. Peak *b* in the self-unfolded XAES of sample 2 is practically absent, and for sample 3 it is displayed only as a weak inflow. Maximum d' grows more dynamically, than in SXS, when temperature of annealing increase. The maxima *b* and d' intensity for the sample 6 (Fig. 15) even exceeds that of the maximum *d* corresponding to the dominant DOS feature. In the self-unfolded XAES of all GC samples maximum π is distinctly resolved and its intensity in comparison with the intensity of the main maximum changes nonuniformly. In SXS (Fig. 12) the feature *a* is appreciably displayed only for the samples 4 and 6, and for the sample 6 this maximum is weaker, than in the sample 4 spectrum. The more pronounced sensitivity of XAES to surface states and influence of different number of

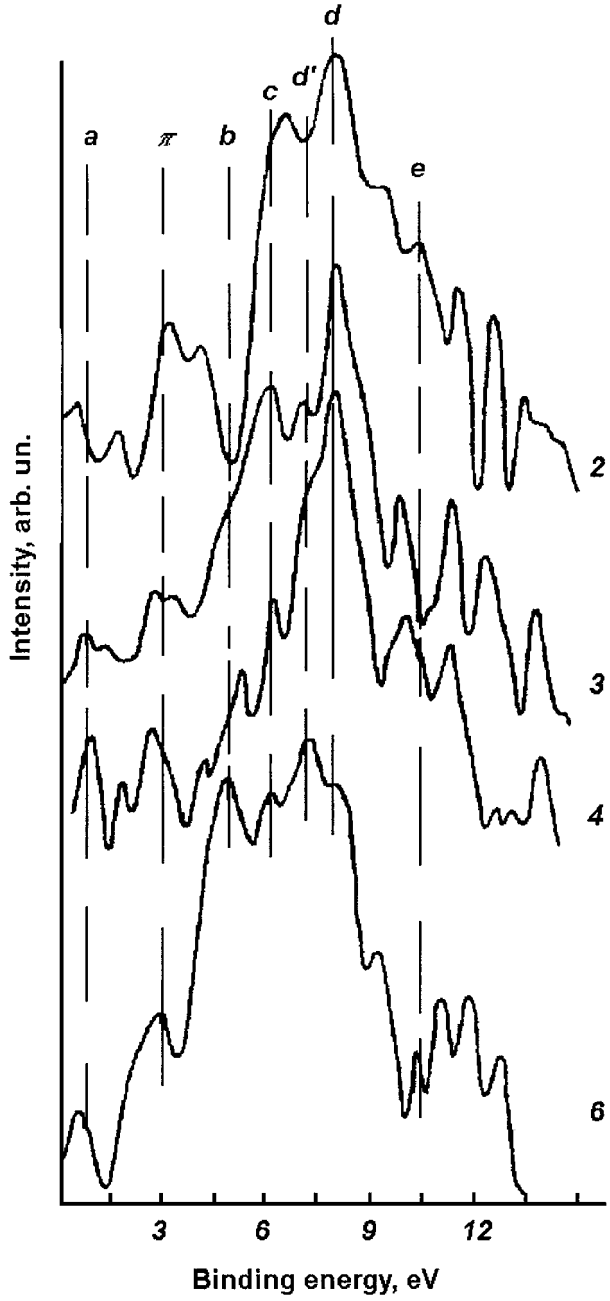

Figure 15 XAES of GC samples heat treated at 1500, 2000, 2500 and 3000°C (accordingly curves 2, 3, 4, 6) after the inverse self-folding treatment.

electronic vacancies in final states of Auger process and K-photoionization on the valence band electronic structure can be mentioned among the probable reasons of such differences in the spectra shapes.

The increase of maximum d' intensity with growth of annealing temperature confirms a conclusion about an increase of the interstitial carbon atoms concentration during GC heat-treatment.

XAES were registered from two various surfaces of the sample 6 when carrying out this research. One of them was prepared by mechanical destruction of a superficial layer to 0.3 mm in depth with the help of a diamond scraper, thus it lost mirror shine, which is characteristic for GC. The opposite side of the sample was not modified in any way except rinsing in acetone. The XAES measurements have shown some spectral features clearly indicating non-equivalence of electronic structure of the both surfaces. The abrased side of the sample manifests a general qualitative similarity to poorly ordered graphite-like systems. The other one has the features intermediate between these of the former and carbyne-like carbons [80] thus confirming the absence of a highly graphitized film on a GC surface. These data bring a new puzzle about the origin and nature of GC superficial layer.

4.2.4. The core electrons XPS

In [68] along with GC samples 1–4, 6 (see Introduction) a sample of highly oriented pyrolytic graphite (HOPG) was investigated as a testing object. The received core electron spectra, normalized on height of a main maximum, are given in Fig. 16. The spectra consist of actually C*1s*-peaks and of rather intensive wide satellites. The spectra of satellites are displayed in increased scale in the figure. From Fig. 16 it is clearly seen that the change of GC annealing temperature changes energy positions of C*1s*-peak and its satellite (curves 1–4, 6 according to numbering of the samples). A HOPG spectrum (curve G) contains a pronounced feature at binding energy about 291 eV, which is characteristic of graphite and hydrocarbons and originates from π-electrons excitation [71].

The data on energy position measured with accuracy 0.1 eV, half-height-width (HHW) and the asymmetry index of C*1s*-lines of the investigated samples are placed in Table VI.

The data of the Table VI show that the binding energy appropriate to a maximum of C*1s*-peak position

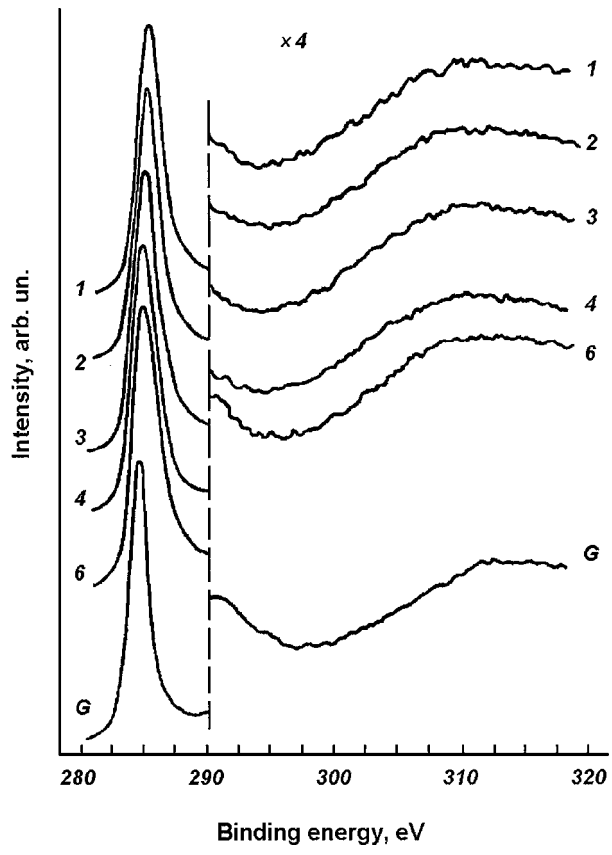

Figure 16 The core electrons XPS of GC samples heat treated at 1200, 1500, 2000, 2500 and 3000°C (accordingly curves 1, 2, 3, 4, 6) and of HOPG (curve *G*).

TABLE VI *C1s*-line parameters of the samples investigated

Sample	Maximum position (eV)	HHW (eV)	Index of asymmetry
1	285.5	2.14	1.33
2	285.4	2.14	1.32
3	285.2	2.21	1.28
4	285.0	2.09	1.39
6	285.0	2.22	1.53
HOPG	284.5	1.55	1.42

monotonously decreases with increase of GC annealing temperature not reaching a value, characteristic of graphite. HHW of the core lines changes non-monotonously, remaining essentially greater than that of HOPG. The asymmetry index of a line was measured as the ratio of the areas of spectra in a binding energy interval 5 eV to the right and to the left from an energy position of a main maximum after a subtraction of a constant component of a background. The asymmetry index also changes non-monotonously, and for the sample 6 it is even more than for HOPG.

As it was already marked above, the survey spectra have shown that the only impurity in appreciable amount contained on a surface of samples was oxygen. The formation of chemical bonds of carbon atoms with the oxygen containing groups results in shift of C*1s*-lines to the higher binding energy values [71]. Hence, it should increase an asymmetry index of the effective spectra, which represent a superposition of the contributions of the core electrons passed in the detector. The same effects should also result in the spectrum broadening.

However, analysis of survey spectra has shown that the sample 6 surface contained approximately 30% less of oxygen than the sample 1 one. At the same time HHW and core line asymmetry of the sample 6 is greater than those of the sample 1 (see Table VI). Hence, the distinctions of these parameters of C*1s*-lines for various samples are determined not only by chemical absorption, but also by changes of GC crystal structure due to high-temperature heat treatment.

Among of probable mechanisms influencing to parameters of core lines may be an increase of delocalized electrons number with GC annealing at the expense of reduction of boundary atoms relative yield (or, in other words, due to a growth of layers), which act as the traps of π-electrons. It results in increase of π-excitations intensity (about 6.5 eV from a core peak) that increases an asymmetry index. On the other hand, the development of mobile π-electronic system reduces the time of core holes relaxation and, hence, increases a natural width of a line.

Thus, the reduction of absorbed oxygen amount during annealing well explains just the changes of C*1s*-line energy position (see Table VI). However one cannot exclude an influence of the local crystalline field variation with layer growth as a result of GC heat treatment.

The annealing of samples appreciably changes the shape and intensity of C*1s*-line satellite spectra existing from the side of high binding energy. The total width of them in the investigated interval was of the order 33–34 eV. The nature of these spectra has a complex char-

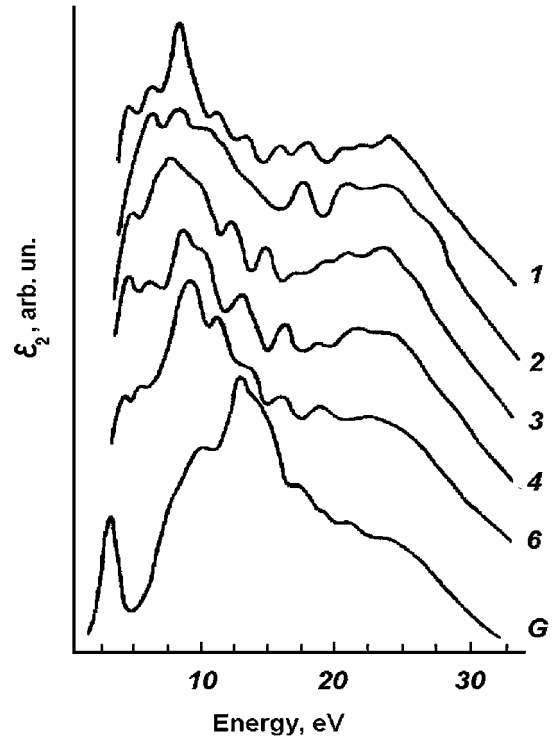

Figure 17 The dependence of the imaginary part of loss function on energy loss derived from the data of Fig. 16.

acter. Those of C*1s*-electrons the escape of which is accompanied by numerous inelastic processes form them. Among these processes are both one-electron and multiple effects: band-to-band transitions, excitations of plasmons, static and dynamic screening, "shake-up" of a valence system by a core hole and so on [48]. In solids their interaction with electromagnetic radiation causes a qualitatively similar response. The energy distribution of the satellites fine structure reflects the features of characteristic losses and should qualitatively correspond to optical spectra of absorption, that allows to carry out similar phenomenological treatment of spectra of both types [83]. The standard Kramers-Kroenig analysis was applied in [68] for spectra of satellites after subtraction of "genuine" C*1s*-peak and smoothing. The algorithm of treatment was similar to the previously used in [83]. The real (ε_1) and imaginary (ε_2) components of a complex dielectric function with the assumption of zero "absorption" at the edges of the energy range 0–33 eV were found. This assumption seems to be justified by the analysis of actually optical results for carbons [84].

The results of ε_2 evaluation for the samples investigated in [68] are present in Fig. 17. The origin of an energy scale coincides with a position of a C*1s*-line maximum for each sample. We consider the basic elements of spectra ε_2 structure in relation with band-to-band transitions and plasma oscillations. The result obtained for HOPG (curve G) are in excellent accordance with the data in [83]. The given below brief analysis of this curve shape is based on the assumption, that multiple shake-up of a valence system by a core hole insignificantly distorts an initial "one-electron" band. The basic fine structure features at 3, 10, 12 and 17 eV correspond to transitions $\pi \to \pi^*$ (M), $\pi \to \sigma^*$ (M), $\sigma \to \sigma^*$ (Γ) and $\sigma \to \pi^*$ (M). The symbol "*" means

free electronic states of σ- and π-symmetry, M and Γ are the characteristic points of a graphite Brillouin zone in which a combined density of occupied and free states is the highest [85].

It follows from Fig. 17 that the main differences of GC satellite structure (curves 1–4, 6) from graphite one (curve G) manifest in displacement of the basic peaks of absorption to smaller energy values, and also in the increased absorption at 22 eV.

The results reported in [44, 46, 66, 67] bring to an assumption that the main difference of GC electronic structure from that of graphite is the existence of additional free energy bands close to the Fermi energy. The occurrence of these bands is connected to the specific energy condition of boundary atoms of carbon layers [19, 28] and carbon atoms intercalated between layers (interstitials) [66, 67]. It creates an opportunity of transitions in these free states at smaller characteristic shake-up energy, that is the reason of the shift of the basic maxima in ε_2 GC spectrum in the direction of smaller energy values [68].

The peak of absorption at 22 eV corresponds to the collective electronic oscillations in carbynoids [86]. With increase of number of a sample the intensity of this peak decreases, that testifies to reduction of a chained component in GC structure with growth of the annealing temperature and qualitatively accords with the results of [34, 38].

4.2.5. Inverse photoemission spectra

The method of the inverse photoemission spectroscopy (IPES) within last decades is frequently used for the researches of unoccupied states of various carbons [see, for example, 87, 88]. However among them there are no works on GC study. But, according to [48, 50], there exist the additional free states generated by carbon atoms introduced between graphite-like layers. Thermoelectricity data [44] show that the concentration of the interstitials grows with increase of annealing temperature. So IPES seem to be helpful to reveal these states, which can be considered as an additional confidence of the self-intercalation process.

In 1994 together with A. V. Solonin, V. L. Kuznetsov, O. B. Sokolov and I. V. Gribov the author carried out measurements of IPE spectra of two GC samples (samples 2 and 6, see Introduction). The pump system allowed to reach oil-free vacuum not worse than 10^{-8} Pa.

For calibration of spectra of carbon samples the IPES of nickel and silver were also measured. A spectrum of silver gives the possibility to determine the spectrometer resolution (0.7 eV). As the density of states in carbons close to the bottom of a conduction band is small there arises difficulties in definition of the Fermi level position. To avoid them the following technique was used. On the holder of samples the nickel sample was placed slightly above the researched carbon one. After the spectrum of each carbon registration the holder moved down in a vertical direction so that the nickel target got the same position (to within 0.1 mm) in which originally a carbon sample was situated.

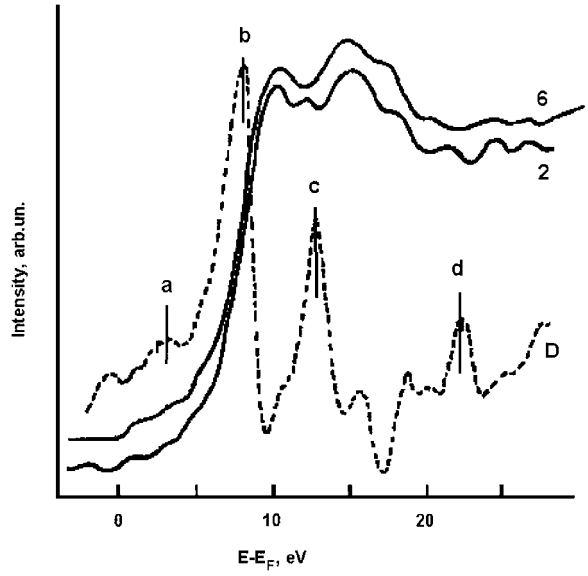

Figure 18 Inverse photoemission spectra of GC samples, heat treated at 1500 and 3000°C and their difference spectrum (accordingly curves 2, 6 and *D*).

Before installation in vacuum system the samples were exposed to careful mechanical scratching. The IPE spectra scanning for each sample was made repeatedly that has allowed to be convinced of good reproducibility of the results. The spectra shape did not change due to long influence of an electron beam that testifies to the absence of a surface modification during registration. The control XPS and XAES scans also have shown that the form and the energy positions of spectral features before and after IPE measurements are identical.

In Fig. 18 the IPE spectra of the two investigated GC samples (HTT = 1500 and 3000°C) are displayed (curves 2 and 6 are designated according to the common numbering, see Introduction). The spectra are normalized to the height of the main maximum. Their Fermi level positions coincide and are accepted as an energy scale origin. The IPE spectra shape of GC samples 2 and 6 are consistent with the experimental data for polycrystalline graphite [88]. The broken curve D in Fig. 18 represents a difference of spectra 6 and 2 and corresponds to those states of unoccupied band, which do exist in sample 6, but are absent in sample 2. Though the shape and the energy position of the difference spectrum are repeatedly reproduced in various series of experiments, nowadays it is impossible to define with confidence a nature of these states. However even the fact of their presence specifies an essential influence of high-temperature annealing on the character of atomic arrangement and electronic structure of GC. This influence is unlikely to be reduced only to quantitative changes, but results in deep qualitative transformations of structure of this unique carbon material.

5. The structural models of GC

5.1. The existing models

The above review of various properties of GC allows to consider their correspondence to the existing models of its structure. The images received in [1] agree well with a model of microstructure, which fragment was given in Fig. 1. Jenkins and Kawamura [1, 20] were the first

to "launch" this structural model: entangled stacks of long but narrow graphite-like layers. The results of GC electron microscopy obtained by Bose and Bragg [21] also gave further confirmation to this model.

Fedorov *et al*. [89] have developed a qualitatively contrary structural model on the basis of a set of electron microscopy, X-ray diffraction and chemical data. According to this model GC macroscopic structure is not uniform, but has a bi-phased character. The superficial film has a layered structure and is able to graphitize. The spherical particles (globules) have diameters of 12–40 nm and form the volume of a sample providing its thermal stability. The concentric spherical layers forming a globule surface are not ordered in relation to crystallographic axis *c* (a turbostratic structure). Fedorov *et al*. [89] consider Jenkins and Kawamura's model as a special case of a globular one: the images of atomic planes in [1, 20] are the sections of globule surface, destroyed during a preparation of GC samples for the transmission electron microscopy. Model [89] well explains uniformity, impermeability to gases and stability of structure under annealing. The coherent scattering areas according to this interpretation are quasi-smooth sites on a globule surface. However the calculated interference function for a model spherical stack with diameter 5 nm, made of 12 layers [89] much worse fits to experimental one, than for a model of flat rectangular layers [12]. Besides, as it was shown above in Section 4 of this review, the measurements of Auger spectra testify that the electronic structure of GC surface differs significantly from that of graphite. This fact makes the assumption about an existence of a graphitizable superficial film ambiguous in general. Nevertheless, the creation of graphitizable areas in GC under influence of catalysts [90] and first of all on a sample surface is rather probable. That could result in a conclusion about existence of such a film from the data on interaction of GC with platinum [90]. Moreover, in a number of X-ray and electron diffraction studies [24, 25, 91, 92] the inclusions, which reflections corresponded to monocrystalline graphite were really found in GC! Yamaguchi [35] has observed partial graphitization of GC at high HTT for a thin (0.06 cm) and highly porous sample. The last effect has received an explanation only after 11 years in [93], where with the help of measurements of physical properties the influence of GC density on their ability to partial graphitization after annealing owing to internal stresses arising due to thermal expansion was shown. Khakimova *et al*. [94] also proved the increase of GC ability to partial graphitization with milling.

A series of papers by Kotosonov and co-workers [see, for example, 95, 96] is devoted to the influence of mechanical pressure and doping on GC structure and physical properties. It has been shown, that the application of external mechanical pressure during synthesis, as well as introduction of doping species result in deeper rearrangement of GC crystalline structure which becomes more similar to that of graphite.

The "globular" model [89] also fails to explain durability and hardness of GC. In the volume of a sample the interaction between the globules can occur only by means of basic surfaces of layers. Such interaction is much weaker than that of atoms inside a layer and cannot ensure GC observable mechanical properties.

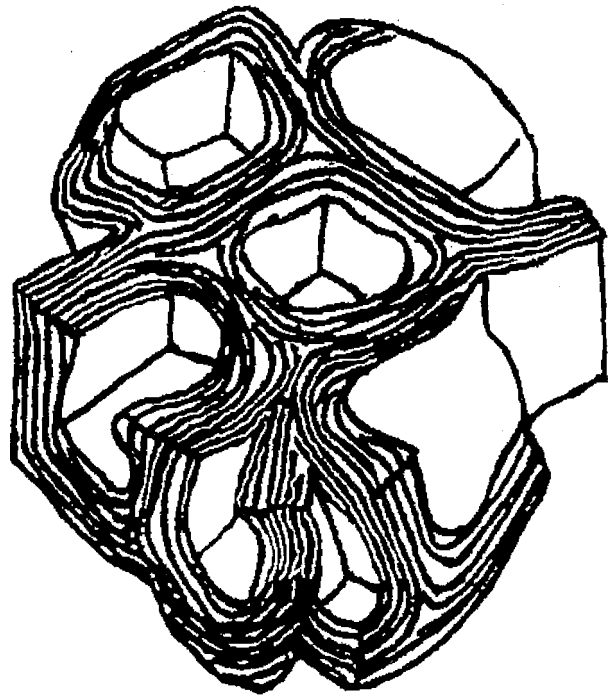

Figure 19 A model for microtexture of hard carbon heat treated at high temperature (from [5, 39]).

Similar to the just above discussed, but more realistic models of GC structure were advanced by Oberlin *et al*. [see, for example, 2, 8, 97, 98] and Shiraishi [3, 5, 39]. According to them the form of the stacks of aromatic layers is isometric, but not ribbon-like. The reason of non-graphitizability is purely in structural geometry: the packs of layers cannot grow more than a pore wall thickness, which is rather small. In turn, the latter is defined by an average diameter of mesophase areas at GC carbonization stage (∼5 nm). Just at this stage the external mechanical pressure modifies properties and structure of GC in the most effective way [95]. GC annealing results in straightening of crumpled packs of graphite sheets, and simultaneous increase of pores size and CSD. This model is displayed in Fig. 19 taken from [5, 39].

This model is entirely alternative to that one developed in [1] (see also Fig. 1). It is in good agreement with many experimental results submitted in the present review, and, in opinion of a number of the authors [see, for example, 39, 99], is more preferable for the correct description of GC structure and properties.

However, a large amount of electronic microphotos [1, 13, 100] evidently show the motive of structure (rotational moires, Fig. 15 from [8]) schematically plotted in Fig. 20. This seems to correspond better to the model of entangled carbon laths, which width is significantly less than their real length.

Some of the data available from literature could be interpreted successfully by both of the models [1, 20] and [97–98], for instance, the measurements made by Wignall and Pings [26]. Microphotos obtained by Yoshida *et al*. show, that the grains have obviously visible rounded configuration [39]. For interpretation of this fact structural models of GC advanced by Oberlin

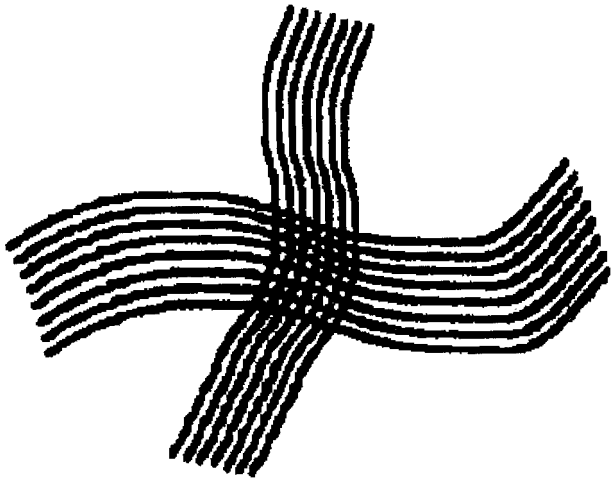

Figure 20 A scheme of the GC structural motive (crossing graphite-like fibrils) observed by means of scanning transmission electron microscopy (STEM) technique [1, 13, 100].

and Shiraishi were used [39]. However similar character of GC texture can also be treated as "rolls" of tangled ribbon-like fibril conglomerates [101].

Hence, from the above part of this review it becomes clear, that structural models of GC, alternative to "fibril" one by Jenkins and Kawamura [1, 20], cannot explain the whole variety of the experimental results. However, the last model is naturally not universal either. In particular, it does not take into account the possibility of the existence of structural fragments having the type of hybridization distinct from sp^2, for example, due to variations of the interatomic bonds length and valence angles [16, 17], chemical linkages, twisting of structural elements [102], edges of layers, presence of interstitials and other structural defects of various origin, but not only folding of ribbons.

Fialkov [5] assumes, that carbon-carbon bonds of 0.155 nm in length, found out in GC alongside with graphite-like ones [18] are not tetrahedral diamond-like bonds but are originated from hexagonal planes deformation. He explains the washing out of diffraction lines by a large variety of interatomic spaces in GC.

In [103] the study of radial distribution of electronic density function was carried out. These results have shown, that in GC are available chained (carbyne-like) carbon structures with interatomic bonds having average length of 0.128 nm. The amount of atoms in chains has appeared to be of the same order as that of atoms forming layers, and with increase of HTT it changes non-monotonously. The presence of chain-ordered structural fragments in GC is also suggested in [68, 104].

The one-dimensional carbon structures have unusual physical properties owing to the specific features of crystalline and electron structure [105]. Therefore chained components in GC structure, quantity and state of which depends on annealing temperature, can essentially influence its electronic structure and physical properties. The coexistence in GC of one- and two-dimensional structures is in accordance with modern views on a structure of carbon bodies [6] and, as we saw above, proves to be true by the electrical conductivity studies [34]. The carbon chains are absent in the existing models of GC structure.

Hence, the complexity of GC electronic structure and atomic order results in impossibility of the description in general of its physical properties with the help of the existing models.

5.2. A new structural model of GC and its heat-treatment behaviour

Recently the integral intensity of electronic emission spectra has been found sensitive to the character of carbon valence state hybridization [86, 106]. This gives an opportunity to use this spectroscopic parameter for investigations of GC structural transformations as a result of high-temperature annealing.

We have analysed relative integral intensities of the valence and core XPS and XAES (C*KVV*) of samples 1–4, 6 (see Introduction). Integral intensity of the spectra were measured after subtraction of a constant component of a background equal to the intensity of a spectrum at a threshold value of binding energy; the intervals of integration for valence XPS and XAES were accordingly 23 and 45 eV. The double area of an "elastic" part of C*1s*-peak of each sample was used as internal normalizing standard of intensity. In all cases the spectrometer passing function [70] was taken into account. The identical data were received for HOPG to compare.

The normalized integral intensities of valence XPS (I) and XAES (S) demonstrate opposite behaviour versus annealing temperature (Table VII). This contradicts the results [86, 106] where the growth of both parameters in a sequence carbyne-graphite-diamond was observed, but qualitatively agrees with experimental results on ion irradiation of HOPG [107] and impurity effects [108].

The found out discrepancy may be caused by a number of the reasons. The increase of the yield of wide layers [19] occurs at the expense of destruction of narrower and/or chained structures [68]. That increases the hybridization degree owing to increase of effective number of atoms in the first coordination sphere [106]. A similar effect should be expected also due to formation of interlayer inclusions. The competing influence renders reduction of graphite-like layers distortions both as a result of their size increase and owing to decreasing of oxygen content on the surface. Therefore, the opposite changes of parameters I and S at annealing may reflect

TABLE VII The normalized integral intensity of valence electron XPS (I) and XAES (S), energy position of the XAES first derivative maximum relatively to Auger threshold value (E_A) and the effective number of $2p$-electrons (x) in hybrid bonds

Material	Annealing temperature (°C)	I (10^{-2}, arb. units)	S (10^{-2}, arb. units)	E_A (eV)	x
	GC				
	1200	11.6	60	15.9	1.66
	1500	9.2	63	14.9	1.71
	2000	7.2	77	15.8	1.95
	2500	8.3	66	13.1	1.76
	3000	7.9	70	12.6	1.83
	HOPG				
	3000	7.6	80	11.3	2.00

their different sensitivity to the competing factors influencing hybridization character and to the thickness of an analysed layer of a surface. These effects create essential difficulties with their joint interpretation. It is worth mentioning that the minimum value of parameter I in carbon fibres, a material similar to GC due to the presence of fibrous structural elements [109], was observed just at annealing temperature 2000°C [86] as well as in our experiments (Table VII).

A special study showed that parameter S is expected to reflect hybridization effects in a more reliable and precise manner than I due to the direct and strong influence of heteroatom photoelectron yield on the intensity and shape of XPS [108].

The results of the S parameter measurement and the data from [106, 108] bring to the conclusion that the yield x of wave functions having $2p$-symmetry in the hybrid valence state sp^x has a general tendency to increase due to annealing. This effect is not monotonous: at 2000°C despite the microcrystalline character of the structure [19] the effective hybridization degree in this sample suddenly becomes close to that of graphite (Table VII). This fact as well as the measurements of the main maximum of the XAES first derivative energy position E_A (Table VII) indicates the complex manner of GC electronic structure modification caused by a high-temperature heat treatment. Several other non-monotonous effects were revealed as well. So, both in valence electron XPS and XAES the intensity ratio of the spectrum itself and its background has a maximum accordingly at 2000 and 2500°C. The specific heat capacity measured near room temperature by a calorimetric method has a broad minimum in the HTT range between 2000 and 2500°C. This proves the bulk character of the discussed process of GC structural modification. A number of the experimental data can be explained by the introduction of carbon atoms between growing graphite-like layers with annealing. Simultaneously there occurs a reduction in relative yield of one-dimensional (chain-like) structures. So the assumption that both growth of layers and interlayer inclusion formation are the result of disintegration of chains seems quite reasonable. Indeed, it is the basis for the following model of GLC atomic structure and its evolution upon annealing.

During pyrolysis of thermosetting resins areas of dominant orientation (domains) of aromatic, aliphatic and/or carbyne-like chains reflecting a spatial arrangement of initial polymer chains are formed. These domains make up a set of randomly linked fragments. As a crude first approach one can suppose that each domain has axial symmetry (Fig. 21). Near the central axis of a domain the degree of mutual orientation of chains is so great that some of the adjacent chains join forming a domain nucleus as a result of thermal fluctuations of chain shape and interchain distances. So the nucleus is, apparently, a stack of graphite-like narrow layers (fibril), whose cross section must be significantly smaller than a domain (or chain-like matrix) diameter. The fluctuation nature of this process results in exponential character of the size distribution of graphite-like layers [19]. A main factor determining such system behaviour under

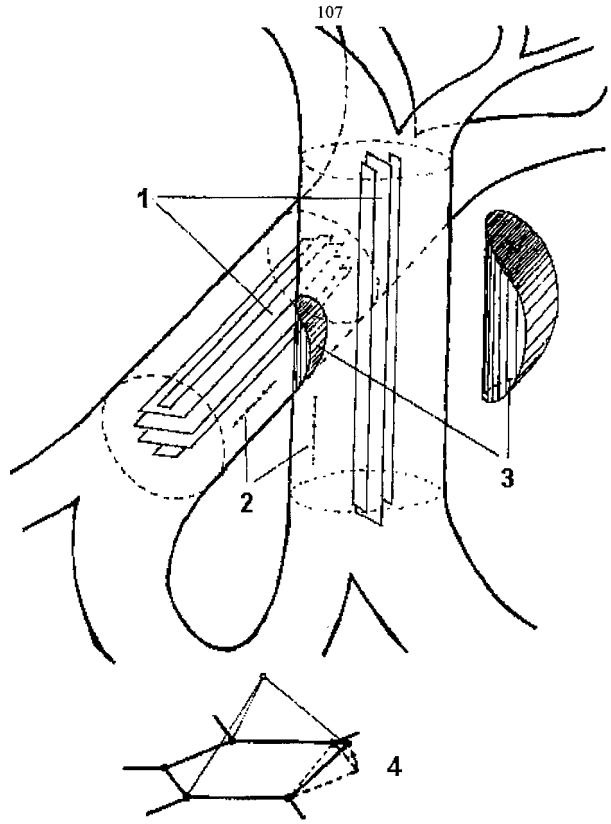

Figure 21 The fibril-and-chained model of GC structure: (1) graphite-like fibrils, (2) carbyne-like chains, (3) a region of non-collinear chains coexistence, (4) a scheme of a displacement of the peripheral atom out of a layer plane as a result of interaction with an interstitial atom.

heat treatment is mutual parallelism of layer edges and the adjacent chains. The increase of annealing temperature initiates growth of fibril layers due to thermal kinks of the chains neighbouring to their prismatic sides and σ-bonding with them. The increase of layer width is accompanied with their mutual rapprochement [110]. The latter is observed as a shift in the angular position of the (*002*) X-ray reflection.

Despite a probable affinity of the domain shape to the cylindrical form, the graphite-like layers should be rather flat. This happens because of the greater thermodynamic stability of such type of ordering in the related area of the carbon phase diagram [27] and the quasi-static thermal influence revealed by us in the course of the annealing of the investigated GC samples. Distortions are most likely present near the periphery of the layers due to valence angle variations, or, in other words, due to hybrid states of peripheral atom distinct from sp^2. In our opinion, strongly non-equilibrium conditions during GC synthesis (for example, a thermal shock and a subsequent fast cooling may result in the symmetry of the layer stacking repeating that of the domains. Thus the microstructure of such carbon will appear as a system of tangled carbon tubes of various diameters. This material is expected to have prospective scientific and technical applications.

Let us consider behaviour of two adjacent domains with non-collinear symmetry axes (Fig. 21). Some pairs of domains can be located so close to one another that their diameters exceed the shortest distance between

central axes. This means the presence of areas where carbon chains oriented in the non-collinear manner coexist. On annealing, graphite-like layers reach the borders of this area as a result of increase of their width and continue to grow owing to chained elements of structure oriented approximately parallel to them. Thus the chains oriented non-collinear to layers get inside a fibril and break up with formation of interstitials. This limits the mutual rapprochement of the layers in fibrils, that is displayed as a weakening of the decrease of the mean interlayer distance with HTT, or even as a weak increase of d_c [13].

As far as modification of the hybridization character with annealing is concerned, the described process occurs in the following way. Over a general tendency of monotonous transition of atoms from *sp*- to sp^2-state at 2000°C there arises an additional increase of hybridization degree due to the overlapping orbitals of out-of-layer and interlayer atoms resulting in sharp increase of the XAES normalized integral intensity (see Table VII). One of the important reasons of this effect is the deformation of a layer near its edge: the bonds formed between out-of-layer and peripheral atoms displace the latter out of the layer plane (Fig. 21). This effect is displayed more weakly in the interaction of an interstitial atom with intralayer atoms having three neighbours. Just for that very reason the hybridization degree and parameter *S* (see Table VII) is less with further annealing and growth of layers than at 2000 C: though the concentration of interstitials continues to grow, their relative quantity near edges of layers decreases. The transition of interstitial atoms into some other state ("strings"), which has a smaller hybridization degree [111], is also probable. One should note that at HTT higher than 2000°C the layers in fibrils are no longer expected to remain flat. The interstitials between graphite-like layers may induce a specific wavy distortion of the layer shape. This is the probable manner of the additional indirect influence of interstitials on the hybridization mode of the in-layer atoms.

The developed model is in accordance with the transmission electron microscopy images of crossing (*002*) planes of various fibrils [1, 13, 100]. It also allows interpretation of various GLC physical properties.

The model itself and our assumptions about the character and tendency of structural transformations in GC contradict at first sight the popular point of view, that due to thermal influence the crystalline structure of carbons becomes less defective (see, for example, [27]). However one should keep in mind an essential feature: the interstitials created directly in low-temperature synthesis of non-equilibrium carbon structures and having the initially significant sizes of isotropic layers (coals, cokes, blacks, pyrocarbons), arise in GC only at a certain layer width and, consequently, at a definite range of annealing temperatures. The formation of these defects occurs at the expense of chain-like fragments disintegration. The chains are initially present in GC structure as "relic" structural elements left from thermosetting resins—the polymeric precursors of GC. The carbon atoms, introduced between the layers, increase GC crystalline structure rigidity in conformity with the well-known inability of GC to transform into graphite due to thermal influence.

6. Conclusions

To summarize our analysis of the data included in the present review, it is necessary to note that despite of the rich history of the glass-like carbon studies, nowadays there is no exhaustive proof of the benefit of a particular model for its structure. This opens a wide field for research activity and for the prospective technological applications of the material. This also stimulates a permanent interest in studying the sensitivity of its physical properties to the structural modifications.

The development of the described above new model of GC structure is also far from complete. The main reason for its ambiguity is the absence of direct experimental proofs of its validity. The most of its features were deduced from the analysis of data that are sensitive to the atomic states in the thin (within a few interatomic distances) surface layer, i.e. XPS and XAES. Besides, there is no evidence that the observed spectral features can originate only from interstitials but not from some other structural distortions. One of the most exciting problems that still remain is the nature of the superficial layer because of the well-established difference of its properties and those of the bulk GC [112, 113]. Our future plans, therefore, include deeper experimental and theoretical studies of the free and occupied electronic states of carbons and the effect of structural defects of various types (including those created artificially to imitate real carbon non-equilibrium structures) on these states.

Acknowledgments

The author greatly appreciates the fruitful discussion of the experimental results on the GC electronic structure with Prof. E. M. Baitinger. The invaluable help of Prof. O. B. Sokolov and Drs. I. V. Gribov, V. L. Kuznetsov, V. V. Romanov, N. A. Mamaev, Mrs. N. A. Moskvina and Mr. A. V. Soloninin in the data registration and discussion is gratefully acknowledged.

It is a great sorrow that this review will never be read by Prof. S. V. Shulepov, a person whom the author always considers as a Teacher. His support and consideration as well as a fair, stimulating criticism, discussions of results and fruitful cooperation have helped the author very much in the initial stage of the GC studies.

References

1. G. M. JENKINS and K. KAWAMURA, *Nature* **231** (1971) 175.
2. A. OBERLIN and M. OBERLIN, *J. Microscopy* **132** (1983) 353.
3. M. SHIRAISHI, "Kaitei Tansozairyo Nyumon (Introduction to Carbon Materials)" (1984) 29 (in Japanese).
4. G. M. JENKINS and K. KAWAMURA, "Polymeric Carbon—Carbon Fibre, Glass and Char" (Cambridge University Press, London, New York, 1976).
5. S. OTANI and A. OYA, *Materials Science and Technology* **9** (1991) 549.
6. A. S. FIALKOV, "Carbon and Carbon Based Intercalation Compounds and Composites" (Aspect Press, Moscow, 1997) (in Russian).

7. V. M. MEL'NICHENKO, A. M. SLADKOV and YU. N. NIKULIN, *Uspekhi Khimii* **51** (1982) 736 (in Russian).
8. E. FITZER, K. MUELLER and W. SCHAEFER, in "Chemistry and Physics of Carbon" (M. Dekker, New York, 1971) p. 237.
9. A. OBERLIN, in "Chemistry and Physics of Carbon" (M. Dekker, New York, 1989) p. 1.
10. S. ERGUN, in "Chemistry and Physics of Carbon" (M. Dekker, New York, 1968) p. 211.
11. W. RULAND, in "Chemistry and Physics of Carbon" (M. Dekker, New York, 1968) p. 1.
12. D. B. FISCHBACH, in "Chemistry and Physics of Carbon" (M. Dekker, New York, 1971) p. 1.
13. F. ROUSSEAUX and D. TCHOUBAR, *Carbon* **15** (1977) 55.
14. *Idem*., *ibid*. **15** (1977) 63.
15. D. B. FISCHBACH, *ibid*. **5** (1967) 565.
16. R. R. SAXENA and R. H. BRAGG, *ibid*. **16** (1978) 373.
17. S. ERGUN, *ibid*. **11** (1973) 221.
18. S. ERGUN and R. R. SCHEHL, *ibid*. **11** (1973) 127.
19. T. NODA and M. INAGAKI, *Bull. Chem. Soc. Japan* **37** (1964) 1534.
20. L. A. PESIN and E. D. SEREZHENKO, *Fizika Tverdogo Tela* **31**(4) (1989) 288 (in Russian). [English translation *Sov. Phys. Solid State* **31** (1989) 714].
21. G. M. JENKINS, K. KAWAMURA and L. L. BAN, *Proc. Royal Soc. Lond. A* **327** (1972) 501.
22. S. BOSE and R. H. BRAGG, *Carbon* **19** (1981) 289.
23. V. F. PETRUNIN, V. A. POGONIN, YU. G. ANDREEV, K. P. VLASOV and V. T. IL'IN, *Neorganicheskie Materialy* **18** (1982) 1292 (in Russian).
24. D. F. R. MILDNER and J. M. CARPENTER, *J. Non-Cryst. Solids* **47** (1982) 391.
25. A. G. WHITTAKER and B. TOOPER, *J. Amer. Ceram. Soc.* **57** (1974) 443.
26. *Idem*., In Extended Abstracts and Program of the 11th Biennial Conference on Carbon, Gatlinburg, Tennessee, USA, June 1973, p. 184.
27. G. D. WIGNALL and C. J. PINGS, *Carbon* **12** (1974) 51.
28. S. V. SHULEPOV, "Physics of Carbons" (Metallurgiya, Chelyabinsk, 1990) (in Russian).
29. R. S. GORDENKO and I. D. MIKHAILOV, *Fizika Tverdogo Tela* **13** (1971) 3677 (in Russian). [English Translation *Sov. Phys. Solid State* **13** (1972) 3103].
30. A. G. KHACHATURYAN, *Kristallografiya* **5** (1960) 354 (in Russian). [English Translation. *Sov. Phys. Crystallogr*. **5** (1960) 335].
31. A. I. KITAIGORODSKIY, "X-Ray Structural Analysis of Microcrystalline and Amorphous Objects" (GITTL, Moscow, 1952) (in Russian).
32. V. G. NAGORNYI, in "Properties of Carbon-Based Constructional Materials" (Metallurgiya, Moscow, 1975) p. 15 (in Russian).
33. T. TSUZUKU and K. SAITO, *Jap. J. Appl. Phys.* **5** (1966) 738.
34. D. R. HUNT, G. M. JENKINS and T. TAKEZAWA, *Carbon* **14** (1976) 105.
35. D. F. BAKER and R. H. BRAGG, *J. Non-Cryst. Solids* **58** (1983) 57.
36. T. YAMAGUCHI, *Carbon* **1** (1963) 47.
37. R. R. SAXENA and R. H. BRAGG, *J. Non-Cryst. Solids* **28** (1978) 45.
38. J. M. ZIMAN, in "Principles of the Theory of Solids" (Cambridge University Press, Cambridge, 1972) p. 210.
39. D. F. BAKER and R. H. BRAGG, *Phys. Rev. B* **28** (1983) 2219.
40. A. YOSHIDA, Y. KABURAGI and Y. HISHIYAMA, *Carbon* **29** (1991) 1107.
41. R. R. SAXENA and R. H. BRAGG, *Phil. Mag.* **36** (1977) 1445.
42. Y. HISHIYAMA, M. INAGAKI, S. KIMURA and S. YAMADA, *Carbon* **12** (1974) 249.
43. Y. HISHIYAMA, Y. KABURAGI, D. F. BAKER and R. H. BRAGG, *Tanso* (1987, no 128) 18 (in Japanese, Abstract in English).
44. T. YAMAGUCHI, *Carbon* **1** (1964) 535.
45. L. A. PESIN, in "Physical Properties of Carbons" (ChGPI, Chelyabinsk, 1988) p. 28 (in Russian).
46. K. NOTO, K. SAITO, K. KAWAMURA and T. TSUZUKU, *Jap. J. Appl. Phys.* **14** (1975) 480.
47. V. V. MONAKHOV, in Proceedings of the X-th All-Union seminar "The Theory of Electronic Structure and Properties of Hard-Melting Compositions" Namangan, September 1991) p 49 (in Russian).
48. R. R. HAERING and P. R. WALLACE, *J. Phys. Chem. Solids* **3** (1957) 253.
49. E. M. BAITINGER, in "Electronic Structure of Condensed Carbon" (UrGU, Sverdlovsk, 1988) p. 45 (in Russian).
50. R. H. BRAGG, *Synt. Metals* **7** (1983) 95.
51. C. PRIESTER, G. ALLAN and J. CONARD, *Phys. Rev. B* **26** (1982) 4680.
52. K. KAWAMURA and R. H. BRAGG, *Carbon* **24** (1986) 301.
53. V. I. VOLGA, A. S. KOTOSONOV and E. V. LOGACHEVA, *Tsvetnaya Metallurgiya* (1985) 41 (in Russian).
54. D. B. FISCHBACH and M. E. RORABAUGH, *Carbon* **21** (1983) 429.
55. V. A. IVANOV, L. A. PESIN and V. V. ROMANOV, in "Problems of Solid State Physics: Physical Properties of Carbons" (ChGPI, Chelyabinsk, 1984) p. 27 (in Russian).
56. YU. A. BOBROVNIKOV and A. S. KOTOSONOV, in "Carbon-Based Constructional Materials, Book 13" (Metallurgiya, Moscow, 1978) p. 65 (in Russian).
57. A. PACAULT and A. MARCHAND, *Compt. Rendus* **241** (1955) 489.
58. L. A. PESIN and S. V. SHULEPOV, *Khimiya Tverdogo Topliva* (1982) 129 (in Russian).
59. A. MAAROUFI, S. FLANDROIS, C. COULON and J. C. ROUILLON, *J. Phys. Chem. Solids* **43** (1982) 1103.
60. M. NAKAMIZO, *Carbon* **29** (1991) 757.
61. R. VIDANO and D. B. FISCHBACH, *J. Amer. Ceram. Soc.* **61** (1978) 13.
62. E. FITZER and F. ROZPLOCH, *Carbon* **26** (1988) 594.
63. D. B. FISCHBACH and M. COUZI, *ibid*. **24** (1986) 365.
64. D. G. MCCULLOCH, S. PRAWER and A. HOFFMAN, *Phys. Rev. B* **50** (1994) 5905.
65. R. R. SAXENA and R. H. BRAGG, *Carbon* **12** (1974) 210.
66. F. R. MCFEELY, S. P. KOWALCZYK, L. LEY, R. G. CAVELL, R. A. POLLAK and D. A. SHIRLEY, *Phys. Rev. B* **9** (1974) 5268.
67. E. M. BAITINGER, L. A. PESIN, V. L. KUZNETSOV and O. B. SOKOLOV, *Fizika Tverdogo Tela* **33** (1991) 3153 (in Russian). [English Translation *Sov. Phys. Solid State* **33** (1991) 1781].
68. L. A. PESIN, E. M. BAITINGER, V. L. KUZNETSOV and O. B. SOKOLOV, *ibid.* **34** (1992) 1734 (in Russian). [English translation *Sov. Phys. Solid State* **34** (1992) 922].
69. *Idem*., *ibid*. **35** (1993) 2262 (in Russian). [English translation *Phys. Solid State* **35** (1993) 1124].
70. E. Z. KURMAEV, S. N. SHAMIN, K. M. KOLOBOVA and S. V. SHULEPOV, *Carbon* **24** (1986) 249.
71. O. B. SOKOLOV and V. L. KUZNETSOV, "The Development of the Experimental Abilities of XPS Method Using Magnetic Analyzer" (ChPI Chelyabinsk, 1990) (in Russian).
72. M. P. SEACH, D. BRIGGS, J. C. RIVIERE, S. HOFFMANN, R. R. OLSON, P. W. PALMBERG, C. T. HOVLAND, T. E. BRADY, T. L. BARR, N. S. MCINTYRE, M. T. ANTHONY, P. SWIFT, D. SHATTLEWORTH, P. M. A. SHERWOOD and C. D. WAGNER, "Practical Surface Analysis by Auger and X-ray Photoelectron Spectroscopy" (John Wiley, Chichester, New York, Brisbane, Toronto, Singapore, 1983).
73. A. E. PAVLATH and M. M. MILLARD, *Appl. Spectrosc.* **33** (1979) 502.
74. V. V. NEMOSHKALENKO and V. V. ALYOSHIN "Electron Spectroscopy of Crystals" (Naukova Dumka, Kiev, 1976) (in Russian).
75. M. P. BYTZMAN, K. M. KOLOBOVA, E. Z. KURMAEV, V. N. BEKASOVA and L. V. GORBANEVA, *Carbon* **20** (1982) 293.
76. P. SKYTT, P. GLANS, D. C. MANCINI, J.-H. GUO, N. WASSDAHL, J. NORDGREN and Y. MA, *Phys. Rev. B* **50** (1994) 10457.
77. V. V. KHVOSTOV, V. G. BABAEV and M. B. GUSEVA,

Fizika Tverdogo Tela **27** (1985) 887 (in Russian). [English translation *Sov. Phys. Solid State* **27** (1985) 543].
78. S. I. VETCHINKIN, S. L. ZIMONT, S. V. KHRISTENKO, G. M. MIKHA'LOV and YU. G. BOROD'KO, *Poverkhnost'* (1987) 90 (in Russian).
79. J. E. HOUSTON, J. W. ROGERS, R. R. RYE, J. E. HATSON and D. E. RAMAKER, *Phys. Rev. B* **34** (1986) 1215.
80. D. E. RAMAKER, *J. Vac. Sci. Technol. A* **7** (1989) 1614.
81. YU. P. KUDRYAVTSEV, S. E. EVSYUKOV, V. G. BABAEV, M. B. GUSEVA, V. V. KHVOSTOV and L. M. KRECHKO, *Carbon* **30** (1992) 213.
82. B. E. KOEL and J. M. WHITE, *J. Electron Spectrosc. and Relat. Phenom.* **22** (1981) 237.
83. YU. M. ROTNER, B. I. REZNIK and B. SH. IVANOV, *Poverkhnost'* (1990) 39 (in Russian).
84. E. M. BAITINGER, YU. A. TETERIN and F. F. KUGEEV, *Fizika Tverdogo Tela* **31** (1989) 316. (in Russian). [English translation *Sov. Phys. Solid State* **31** (1989) 2021].
85. V. V. SOBOLEV, "Energy Structure of the Narrow-Band Semiconductors" (Kishinev, 1983) (in Russian).
86. R. F. WILLIS, B. FITTON and G. S. PAINTER, *Phys. Rev. B* **9** (1974) 1926.
87. F. F. KUGEEV, E. M. BAITINGER, YU. A. TETERIN and S. G. GAGARIN, *Khimiya Tverdogo Topliva* (1991) 120 (in Russian).
88. V. DOSE, G. RENSING and H. SCHEIDT, *Phys. Rev. B* **26** (1982) 984.
89. I. KIESER, *Z. Physik* **244** (1971) 171.
90. V. B. FEDOROV, M. KH. SHORSHOROV and D. K. KHAKIMOVA "Carbon and Its Interaction with Metals" (Metallurgiya, Moscow, 1978) (in Russian).
91. YU. S. LOPATTO, V. P. PEREVEZENTSEV, D. K. KHAKIMOVA, L. G. KHROMENKOV and N. N. SHYPKOV, *Neorganicheskie Materialy* **9** (1973) 1708 (in Russian).
92. J. L. KAAE, *Carbon* **13** (1975) 246.
93. S. NEFFE, *ibid.* **26** (1988) 687.
94. K. KAWAMURA and T. TSUZUKU, *ibid.* **12** (1974) 352.
95. D. K. KHAKIMOVA, E. V. MASLOVA, V. A. FILIMONOV, V. K. BUTYUGIN, B. A. SAMSONOV and A. M. SIGAREV, in "Carbon-Based Constructional Materials, Book 7" (Metallurgiya, Moscow, 1972) p. 98 (in Russian).
96. A. S. KOTOSONOV, V. A. VINNIKOV, V. I. FROLOV and B. G. OSTRONOV, *Doklady AN SSSR* **185** (1969) 1316 (in Russian).
97. B. G. OSTRONOV and A. S. KOTOSONOV, in "Carbon-Based Constructional Materials, Book 17" (Metallurgiya, Moscow, 1983) p. 51 (in Russian).
98. A. OBERLIN and M. OBERLIN, *J. Microscopy* **132** (1983) 353.
99. A. OBERLIN, *Carbon* **22** (1984) 521.
100. M. HUTTEPAIN and A. OBERLIN, *ibid.* **28** (1990) 103.
101. J. LACHTER, B. N. MEHROTRA, L. G. HENRY, R. H. BRAGG, *ibid.* **25** (1987) 775.
102. S. BOSE, U. DAHMEN, R. H. BRAGG and G. THOMAS, *J. Amer. Ceram. Soc.* **61** (1978) 174.
103. YU. S. VIRGIL'EV, E. I. KUROLENKIN and T. K. PEKAL'N, in "Carbon-Based Constructional Materials, Book 14" (Metallurgiya, Moscow, 1979) p. 72 (in Russian).
104. A. A. KHOMENKO, YU. E. SMIRNOV, V. P. SOSEDOV and V. I. KASATOCHKIN, *Doklady AN SSSR* **206** (1972) 1112 (in Russian).
105. S. E. EVSYUKOV, in "Carbyne and Carbynoid Structures" (Kluwer Academic Publishers, Dordrecht, The Netherlands, 1999) p. 133.
106. R. B. HEIMANN, J. KLEIMAN and N. M. SALANSKY, *Carbon* **22** (1984) 147.
107. L. A. PESIN, in "Carbyne and Carbynoid Structures" (Kluwer Academic Publishers, Dordrecht, The Netherlands, 1999) p. 371.
108. L. A. PESIN, E. M. BAITINGER, I. V. GRIBOV, V. L. KUZNETSOV and O. B. SOKOLOV, *Fizika Tverdogo Tela* **37** (1995) 2706 (in Russian). [English translation *Phys. Solid State* **37** (1995) 1488].
109. L. A. PESIN, E. M. BAITINGER, I. N. KOVALYOV, S. E. EVSYUKOV and YU. P. KUDRYAVTSEV, *Zhurnal Strukturnoi Khimii* **40** (1999) 493 (In Russian). [English translation *J. Struct. Chem.* **40** (1999) 406].
110. J. W. MCCLURE and B. B. HICKMAN, *Carbon* **20** (1982) 373.
111. E. A. BELENKOV and A. I. SHEINKMAN, *Izvestiya Vuzov. Fizika* **34** (1991) 67 (in Russian) [English translation *Sov. Physics Journal* **34** (1991) 903].
112. M. I. HEGGIE, *Carbon* **30** (1992) 71.
113. A. DEKANSKI, N. S. MARINKOVIC, J. STEVANOVIC, V. M. JOVANOVIC, Z. LAUSEVIC and M. LAUSEVIC, *Vacuum* **41** (1990) 1772.
114. N. IWASHITA, M. W. SWAIN, J. S. FIELD, N. OHTA and S. BITOH, *Carbon* **39** (2001) 1525.

Received 18 January
and accepted 23 July 2001